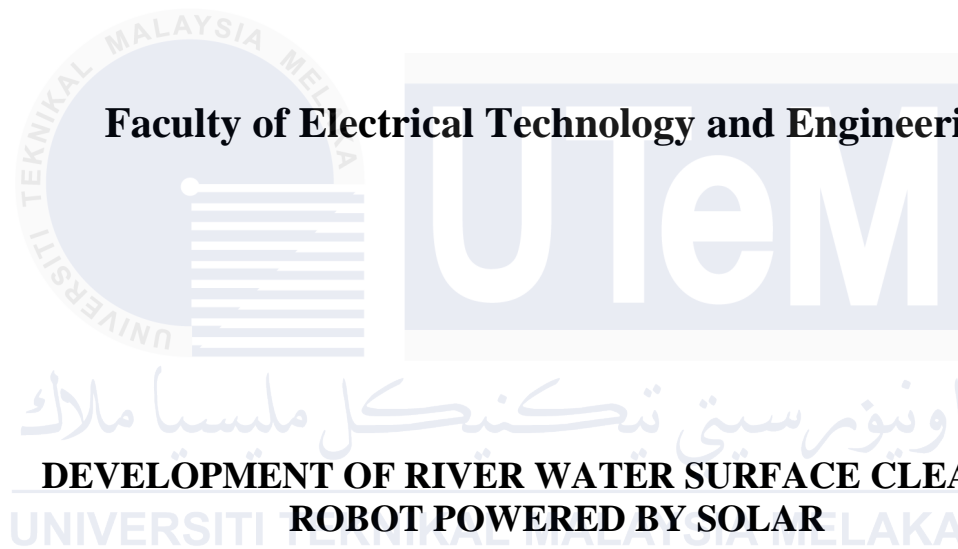




Faculty of Electrical Technology and Engineering



**DEVELOPMENT OF RIVER WATER SURFACE CLEANING
ROBOT POWERED BY SOLAR**

FAIZUL IMRAN BIN SULAIMAN

Bachelor of Electrical Engineering Technology with Honours

2024

**DEVELOPMENT OF RIVER WATER SURFACE CLEANING ROBOT
POWERED BY SOLAR**

FAIZUL IMRAN BIN SULAIMAN



**A project report submitted
in partial fulfillment of the requirements for the degree of
Bachelor of Electrical Engineering Technology with Honours**

اونيورسيتي تېكنيكل مليسيا ملاك
UNIVERSITY OF TECHNOLOGY MALAYSIA MELAKA
Faculty of Electrical Technology and Engineering

UNIVERSITI TEKNIKAL MALAYSIA MELAKA

2024

DECLARATION

I declare that this project report entitled Development of River Water Surface Cleaning Robot Powered by Solar is the result of my own research except as cited in the references. The project report has not been accepted for any degree and is not concurrently submitted in candidature of any other degree.

Signature :

Student Name :

FAIZUL IMRAN BIN SULAIMAN

Date :

4 JANUARY 2025

UNIVERSITI TEKNIKAL MALAYSIA MELAKA

DEDICATION

I dedicate this report to my beloved parents Sulaiman bin Sabikan and Hirne binti Saris. Your support and love have been my strength throughout my years of study. Your belief in me and the sacrifices you made have inspired me to keep moving forward.

To my both supervisor, Arman Hadi bin Azahar and Halyani binti Mohd Yassim, thank you for your guidance and wisdom. You have played a crucial role in shaping my learning and helping me grow as an aspiring engineer.

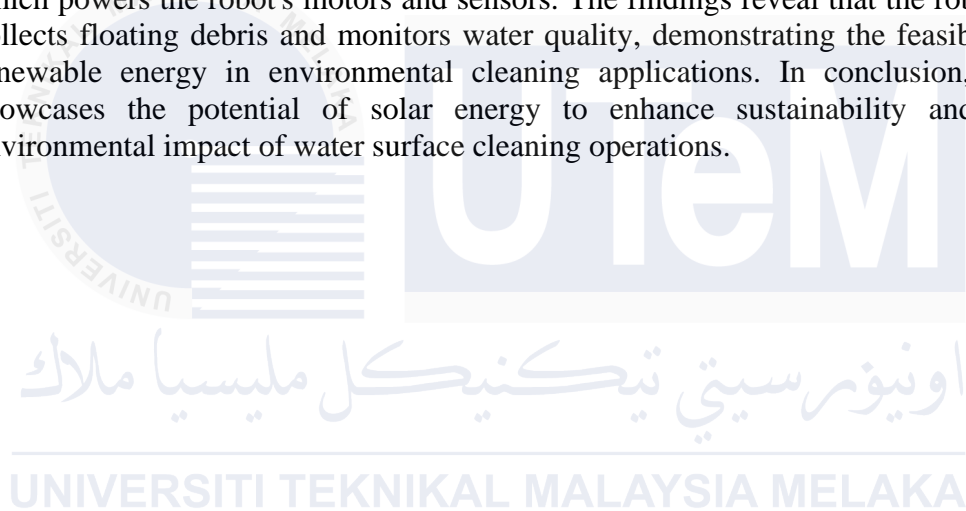
To my friends and colleagues, I am grateful for your encouragement and shared knowledge. Your support has made this journey more meaningful and enjoyable.

Finally, I thank the Almighty for giving me the strength and resilience to reach this milestone. This work is a reflection of all the support and belief I have received along the way.

UNIVERSITI TEKNIKAL MALAYSIA MELAKA

ABSTRACT

This project aims to develop a solar-powered water surface cleaning system to enhance water surface quality and promote environmental sustainability. Water bodies are often polluted by floating debris, which impacts aquatic ecosystems and the environment, and conventional cleaning methods are inefficient and energy-intensive. Therefore, an innovative, energy-efficient solution is needed to address this issue. The objective of this project is to design and develop a solar-powered robot for cleaning water surfaces efficiently while reducing its environmental impact. The project employs an Arduino Uno microcontroller, integrated with a Bluetooth module (HC-05) and an app developed using MIT App Inventor for remote control. An LDR sensor monitors sunlight intensity to optimize solar panel performance, which powers the robot's motors and sensors. The findings reveal that the robot efficiently collects floating debris and monitors water quality, demonstrating the feasibility of using renewable energy in environmental cleaning applications. In conclusion, this project showcases the potential of solar energy to enhance sustainability and reduce the environmental impact of water surface cleaning operations.



ABSTRAK

Projek ini bertujuan untuk membangunkan sistem pembersihan permukaan air berkuasa solar untuk meningkatkan kualiti permukaan air dan menggalakkan kelestarian alam sekitar. Badan air sering dicemari oleh serpihan terapung, yang memberi kesan kepada ekosistem akuatik dan alam sekitar, dan kaedah pembersihan konvensional adalah tidak cekap dan intensif tenaga. Oleh itu, penyelesaian yang inovatif dan cekap tenaga diperlukan untuk menangani isu ini. Objektif projek ini adalah untuk mereka bentuk dan membangunkan robot berkuasa solar untuk membersihkan permukaan air dengan cekap sambil mengurangkan kesan alam sekitar. Projek ini menggunakan mikropengawal Arduino Uno, disepadukan dengan modul Bluetooth (HC-05) dan aplikasi yang dibangunkan menggunakan MIT App Inventor untuk kawalan jauh. Sensor LDR memantau keamatan cahaya matahari untuk mengoptimumkan prestasi panel solar, yang menggerakkan motor dan sensor robot. Penemuan mendedahkan bahawa robot itu dengan cekap mengumpul serpihan terapung dan memantau kualiti air, menunjukkan kemungkinan menggunakan tenaga boleh diperbaharui dalam aplikasi pembersihan alam sekitar. Kesimpulannya, projek ini mempamerkan potensi tenaga suria untuk meningkatkan kemampanan dan mengurangkan kesan alam sekitar operasi pembersihan permukaan air.

ACKNOWLEDGEMENTS

First and foremost, I would like to express my gratitude to my supervisor, Halyani Binti Mohd Yassim and co-supervisor, Arman Hadi Bin Azahar for their precious guidance, words of wisdom and patient throughout this project.

I am also indebted to Universiti Teknikal Malaysia Melaka (UTeM) and Faculty of Electrical Technology and Engineering for the financial support through Development of River Water Surface Cleaning Robot Powered by Solar which enables me to accomplish the project. Not forgetting my fellow colleague, BELT S1/1 for the willingness of sharing his thoughts and ideas regarding the project.

My highest appreciation goes to my parents, and family members for their love and prayer during the period of my study.

Finally, I would like to thank all the staffs at the BELT S1/1, fellow classmates, the faculty members, as well as other individuals who are not listed here for being co-operative and helpful.

TABLE OF CONTENTS

	PAGE
DECLARATION	
APPROVAL	
DEDICATIONS	
ABSTRACT	i
ABSTRAK	ii
ACKNOWLEDGEMENTS	iii
TABLE OF CONTENTS	iv
LIST OF TABLES	vii
LIST OF FIGURES	viii
LIST OF APPENDICES	xi
CHAPTER 1 INTRODUCTION	1
1.1 Background	1
1.2 Problem Statement	3
1.3 Project Objective	5
1.4 Scope of Project	5
CHAPTER 2 LITERATURE REVIEW	7
2.1 Introduction	7
2.2 Renewable Energy	8
2.2.1 Solar Energy	11
2.2.1.1 Monocrystalline Solar Cell	11
2.2.1.2 Polycrystalline Solar Cell	12
2.2.1.3 Thin-Film Solar Cell	13
2.3 Microcontroller	14
2.3.1 Arduino Uno	15
2.4 Storage System	16
2.4.1 Rechargeable Battery	16
2.5 The Impact of pH Levels on Aquatic Ecosystems	17
2.6 Ph Sensor E-201-C	18
2.7 Summary on Development of Water Surface Cleaner	20
CHAPTER 3 METHODOLOGY	26
3.1 Introduction	26

3.2	Methodology	26
3.3	Simulation	29
3.3.1	Circuit Design And Simulation	30
3.3.2	Coding For Simulation	30
3.4	Application For Control Robot	30
3.5	2D and 3D Design	31
3.6	Experiment Setup	32
3.6.1	PVC Pipe Sizing : Buoyancy Test	33
3.6.2	Robot Cleaning Movement and Speed	34
3.6.3	HC05 Bluetooth Signal Limit Distance	36
3.6.4	Effect of Sun brightness, temperature and Humidity toward solar efficiency	38
3.6.5	Motor rotation speed	39
3.7	List of Hardware	41
3.7.1	Arduino Uno	41
3.7.2	L298N Motor Driver	41
3.7.3	Hc-05 Bluetooth Module	42
3.7.4	DC Motor	43
3.7.5	12V Solar Panel	44
3.7.6	Charge Controller	44
3.7.7	Lithium Ion Battery	45
3.8	Summary	46
CHAPTER 4	PRELIMINARY RESULTS AND DISCUSSIONS	47
4.1	Introduction	47
4.2	Results and Analysis	47
4.2.1	Complete Circuit	48
4.2.2	Complete Application	49
4.2.3	Complete 2D and 3D Design	50
4.3	Simulation Result	51
4.3.1	Hc-05 Bluetooth Module	52
4.3.2	Develop App Controller	52
4.3.3	Motor	54
4.3.4	Solar and Storage System	59
4.4	Coding for Robot	60
4.4.1	Motor Command Control	61
4.4.2	Command Code for LDR Sensor	62
4.5	Physical Experiment Result	63
4.5.1	PVC Pipe Sizing : Buoyancy Test Result	65
4.5.2	Robot Cleaning Movement and Speed Result	67
4.5.3	HC05 Bluetooth Signal Limit Distance Result	69
4.5.4	Effect of Sun brightness, temperature and Humidity toward solar efficiency Result	70
4.5.5	Motor rotation speed Result	76
CHAPTER 5	CONCLUSION AND RECOMMENDATIONS	78
5.1	Conclusion	78
5.2	Future Works	79

REFERENCES

81

APPENDICES

87



LIST OF TABLES

TABLE	TITLE	PAGE
Table 2.1 :	Comparison 4 Type Common Rechargeable Batteries	17
Table 2.2 :	pH Value and Voltage[43]	19
Table 2.3 :	Summary on Development of Water Surface Cleaner	25
Table 4.1 :	Result for Motor Simulation	57
Table 4.2 :	Pipe Submerged Result	65
Table 4.3:	Robot Travel Time Results	67
Table 4.4 :	DHT11 Communication Distance Results	69
Table 4.5 :	Solar Panel Efficiency Under Different Environmental Conditions	71
Table 4.6 :	Motor Rotational Speed Results	76

LIST OF FIGURES

FIGURE	TITLE	PAGE
Figure 1.1 :	Malacca River[1]	1
Figure 1.2 :	Statistics of Tourist Arrivals to Malacca in 2019[2]	2
Figure 1.3 :	Cleaning Manual Labor Method[3]	4
Figure 2.1 :	The Graph of Renewable Energy in USA since 1950 to 2023[13]	9
Figure 2.2 :	Renewable energy's share of U.S. consumption in 2010[16]	10
Figure 2.3 :	Monocrystalline Solar Panel[24]	12
Figure 2.4 :	Polycrystalline Solar Cell[24]	13
Figure 2.5 :	Thin-Film Solar Cell[24]	14
Figure 2.6 :	Arduino Uno PinOut[33]	15
Figure 2.7 :	Storage Battery System with Charge/Discharge Control[34]	16
Figure 2.8 :	Quantity Hydrogen Ion and Hydroxide Ion	18
Figure 2.9 :	Relationship Between pH Value and Voltage(V)	19
Figure 2.10 :	Block Diagram of Siddhanna Project[44]	20
Figure 2.11 :	Prototype of the Garbage Collector[45]	21
Figure 2.12 :	Block Diagram of the System[45]	22
Figure 2.13 :	Robot Prototype[46]	23
Figure 2.14 :	Overall view of the positions of all components[47]	24
Figure 3.1 :	Bolck Diagram Project	27
Figure 3.2 :	Overall Project Flowchart	28
Figure 3.3 :	Hardware Project Flowchart	29
Figure 3.4 :	Application Flowchart	31
Figure 3.5 :	Pipe Setup	33
Figure 3.6 :	Floating test with Load	34

Figure 3.7 : Distance Setup	35
Figure 3.8 : Robot Cleaner with Load	36
Figure 3.9 : Bluetooth Distance Setup	37
Figure 3.10 : DHT11 and LDR sensor Setup	39
Figure 3.11 : IR Sensor and DC motor Setup	40
Figure 3.12 : Arduino Uno	41
Figure 3.13 : L298N Motor Driver	42
Figure 3.14 : Hc-05 Bluetooth Module	43
Figure 3.15 : Dc Motor	43
Figure 3.16 : Solar Monocrystalline	44
Figure 3.17 : Charge Controller	45
Figure 3.18 : Lithium Ion Battery	45
Figure 4.1 : Full Complete Circuit	48
Figure 4.2 : Complete Application	49
Figure 4.3 : 2D Project Design	50
Figure 4.4 : 3D Project Design	51
Figure 4.5 : Hc-05 in Simulation Proteus	52
Figure 4.6 : Connectivity Status	53
Figure 4.7 : Button Controller	54
Figure 4.8 : Motor Simulation in Proteus	55
Figure 4.9 : Oscilloscope Connection	56
Figure 4.10 : Command in MIT App Inventor	59
Figure 4.11 : Solar And Charge Controller Simulation in Proteus	60
Figure 4.12 : Motor Command Code	62
Figure 4.13 : LDR Command Code	63
Figure 4.14 : Prototype Water Surface Cleaning Robot	64

Figure 4.15 : Load Weight vs Submersion Depth	66
Figure 4.16 : Graph Load Weight Versus Speed	68
Figure 4.17 : Time vs. Output Voltage	72
Figure 4.18 : Sun Brightness vs. Output Voltage	73
Figure 4.19 : Temperature vs. Output Voltage	74
Figure 4.20 : Humidity vs. Output Voltage	75



LIST OF APPENDICES

APPENDIX	TITLE	PAGE
Appendix A	Full Code For Arduino Uno	87



CHAPTER 1

INTRODUCTION

1.1 Background

In the bustling UNESCO city of Melaka, nestled within its historical charm, flows the enchanting Sungai Melaka, a river that draws tourists and locals alike with its picturesque allure[1]. However, preserving its beauty requires consistent efforts to keep it clean. Sungai Melaka, like many other water bodies such as lakes and pools, faces the common challenge of maintaining its cleanliness despite its expansive size and natural complexity. Figure 1.1 illustrates a typical day at the Malacca River, showcasing the everyday activities and scenery along its banks.



Figure 1.1 : Malacca River[1]

In 2019 , As shown in Figure 1.2, the UNESCO city of Melaka welcomed a total of 18,727,337 tourists, with 13,029,221 domestic visitors and 5,698,116 international tourists, according to data from the Melaka State Government[2]. The necessity of regular cleaning for Sungai Melaka is paramount to ensure it remains a delightful destination for everyone. Yet, the sheer scale of the river presents a formidable task. This challenge extends beyond Sungai Melaka to encompass other water bodies, emphasizing the universal need for effective cleaning solutions.

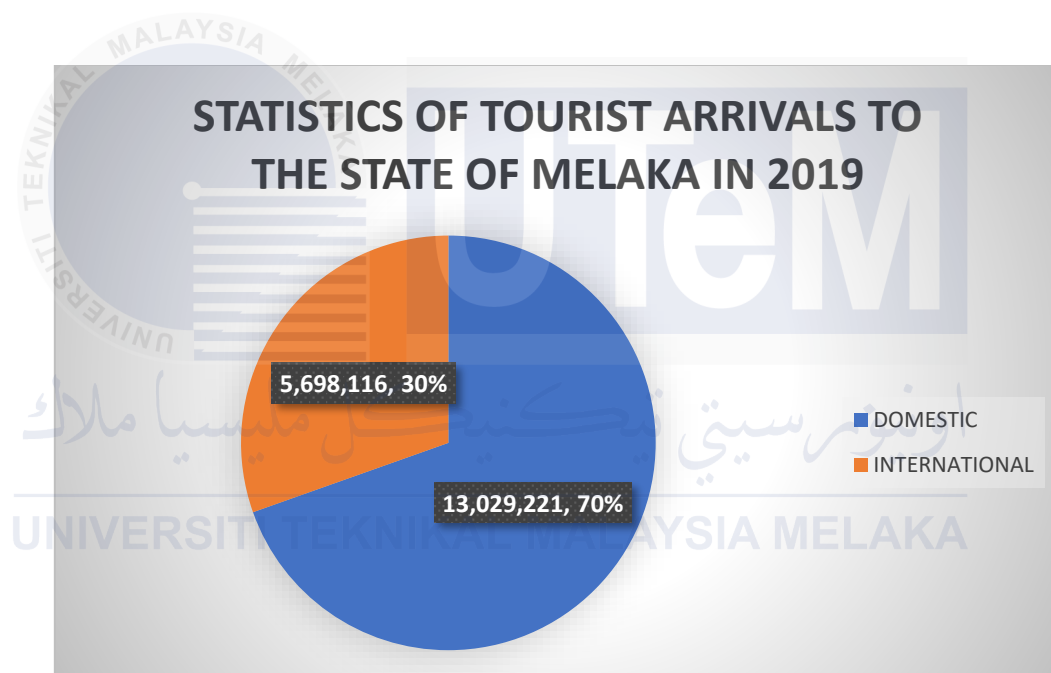


Figure 1.2 : Statistics of Tourist Arrivals to Malacca in 2019[2]

Within this context, the quest for innovations to simplify and enhance the cleaning process gains significant importance. Imagine if solar-powered water surface cleaning robots were deployed along the banks of Sungai Melaka. These robots, powered by clean solar energy, could efficiently collect debris and maintain the river's pristine state, reducing the need for manual labour. This approach not only decreases the reliance on human workers

but also minimizes environmental impact by eliminating the use of fossil fuel-powered machinery.

1.2 Problem Statement

The idea for this project emerged when comparing current methods that rely heavily on manual labour for cleaning water surfaces. Traditional cleaning approaches involve significant human effort, which is not only labour-intensive but also time-consuming and costly. Workers often need to physically remove debris and pollutants from the water, a task that can be strenuous and inefficient, especially given the extensive area and accessibility challenges of water bodies like Sungai Melaka.

The current manual process of hiring motorized boats for water surface cleaning poses significant challenges to efficient and cost-effective environmental maintenance. This process involves recurring tasks of finding and hiring boats, consuming valuable time and incurring substantial financial costs. The need for a two-person team, one driving the boat and the other collecting debris, as shown in Figure 1.3, further increases labour expenses,

limits cleaning frequency, and leads to pollutant accumulation, contributing to environmental degradation.



Figure 1.3 : Cleaning Manual Labor Method[3]

In contrast, employing robots for water surface cleaning presents a more efficient and sustainable solution. Solar-powered cleaning robots can autonomously collect debris and pollutants with minimal human intervention, making use of renewable solar energy. This not only reduces operational costs but also significantly lowers environmental impact compared to fossil fuel-powered machinery. According to research, the energy conversion efficiency of fossil fuels is lower compared to renewable energy sources like solar power. For instance, renewable energy intensity surpasses the efficient use of natural gas and coal energy by approximately 0.51% to 0.37% and 0.43% to 0.17%, respectively[4]. Embracing solar-powered robots not only enhances the efficiency of the cleaning process but also

advances the adoption of green technology, aligning with broader environmental sustainability goals.

The project on developing solar-powered water surface cleaning systems directly relates to Sustainable Development Goal 7 (SDG 7) for Affordable and Clean Energy[5]. Leveraging solar energy to power the cleaning robots promotes the adoption of clean and renewable energy sources. This approach reduces reliance on fossil fuels, mitigates air pollution, and addresses climate change. The use of solar-powered technology aligns with SDG 7's objective of ensuring access to affordable, reliable, sustainable, and modern energy for all.

1.3 Project Objective

The project objective of this project is:

1. To design a water surface cleaning system by developing detailed circuit model that accurately represents the system.
2. To develop a solar-powered water surface cleaning system aimed to enhancing water surface quality and promoting environmental sustainability.
3. To analyze the performance of solar-powered water surface cleaning system by monitoring robot efficiency.

1.4 Scope of Project

The scope of this project encompasses several critical areas for water surface cleaning. These areas include:

- a) **Focus on River Surface:** This project will focus on designing and developing a robotic system specifically for cleaning the surface of rivers.

- b) **Minimal Labor Requirement:** The system will be designed to operate efficiently with only one laborer for monitoring and maintenance.
- c) **Exclusive Use of Solar Energy:** The robot will be powered solely by solar energy to ensure environmental sustainability.
- d) **Integration of Arduino-Controlled Mechanism:** The project will involve designing and building a water cleaning mechanism controlled by Arduino for precise and automated operation.



CHAPTER 2

LITERATURE REVIEW

2.1 Introduction

The rapid pace of technological advancement has brought about a significant paradigm shift in how we approach various tasks, with robotics increasingly replacing manual labour across different domains. Conversely, technological advancements boost production efficiency, lower prices, and drive economic growth, thereby increasing labour demand[6]. This trend is primarily fuelled by the inherent advantages that robots offer, such as increased efficiency and cost-effectiveness. Consequently, tasks that were traditionally carried out by human workers, including river cleaning, are now being reconsidered for automation through the adoption of robotic solutions. Robot adoption tends to have a more significant positive impact in advanced economies compared to emerging ones, potentially widening the gap between it[7].

The focus of this literature review is to delve deeply into the current landscape of robotic river cleaning technology. This involves an exploration of the diverse types of robots utilized for this purpose, ranging from autonomous aquatic drones to remote-controlled submersibles. In construction, machines are already capable of performing tasks like drilling and polishing[8]. However, these basic machines are still unable to fully replace human workers[9]. Additionally, the review will analyze the functionalities of these robots, such as

their ability to navigate water bodies, detect and remove pollutants, and interface with monitoring systems for data collection and analysis.

By thoroughly examining existing research and case studies, the aim is to gain a comprehensive understanding of the efficacy and limitations of robotic system. Despite robots being durable, swift, and precise, capable of outperforming humans in speed, quality, and cost, the human factor remains important in collaboration[10]. This understanding is crucial for assessing their potential role in safeguarding our waterways and addressing the growing concerns of water pollution and environmental degradation. Ultimately, the insights derived from this review will contribute to informed decision-making regarding the adoption and optimization of robotic solutions for river cleaning initiatives.

2.2 Renewable Energy

Renewable energy refers to energy derived from resources that are naturally replenished on a human timescale, such as sunlight, wind, rain, tides, waves, and geothermal heat[11]. This type of energy is considered sustainable and environmentally friendly because it produces little to no greenhouse gas emissions compared to fossil fuels[12]. The United States has seen a marked increase in the use of renewable energy sources, particularly wind and solar, since the early 2000s[13]. The world is beginning to contemplate strategies for reducing air pollution. China has progressively bolstered its policies and initiatives in commitment to the 2009 Copenhagen Accord, as shown in Figure 2.1, aiming to reduce its

carbon dioxide emissions per unit of GDP by 40 to 45% by 2020 from the 2005 baseline level[14].

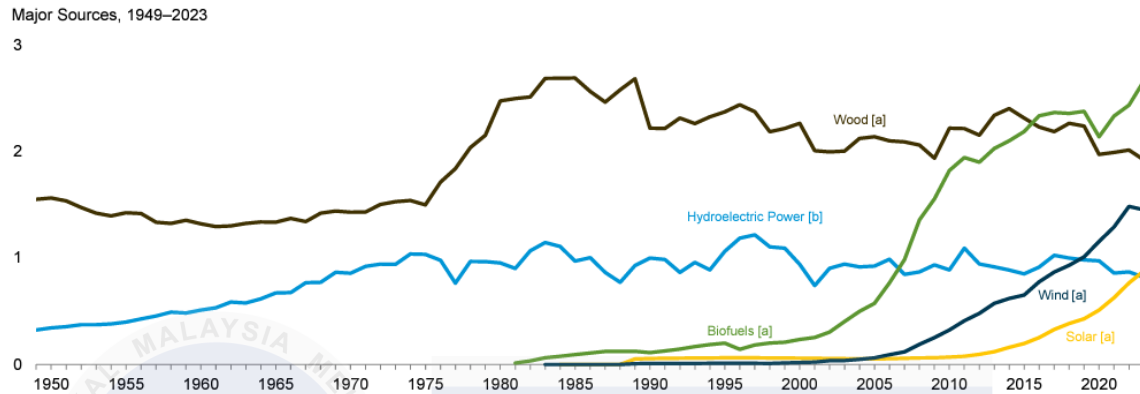


Figure 2.1 : The Graph of Renewable Energy in USA since 1950 to 2023[13]

Fossil fuels have long been the backbone of global energy supply, meeting vast demands across industries and societies[15]. However, their inherent limitations, such as fluctuating prices due to geopolitical factors and finite reserves, highlight the urgency of shifting to sustainable alternatives for stable long-term energy security and environmental preservation. In 2010, the U.S. energy consumption was heavily reliant on non-renewable sources, as shown in Figure 2.2, renewable energy making up a modest 8% of the total energy supply[16]. These finite resources, including coal, oil, and natural gas, are non-renewable and deplete over time, leading to escalating extraction costs and environmental

degradation[17]. Additionally, their combustion releases greenhouse gases, contributing significantly to climate change and air pollution[12].

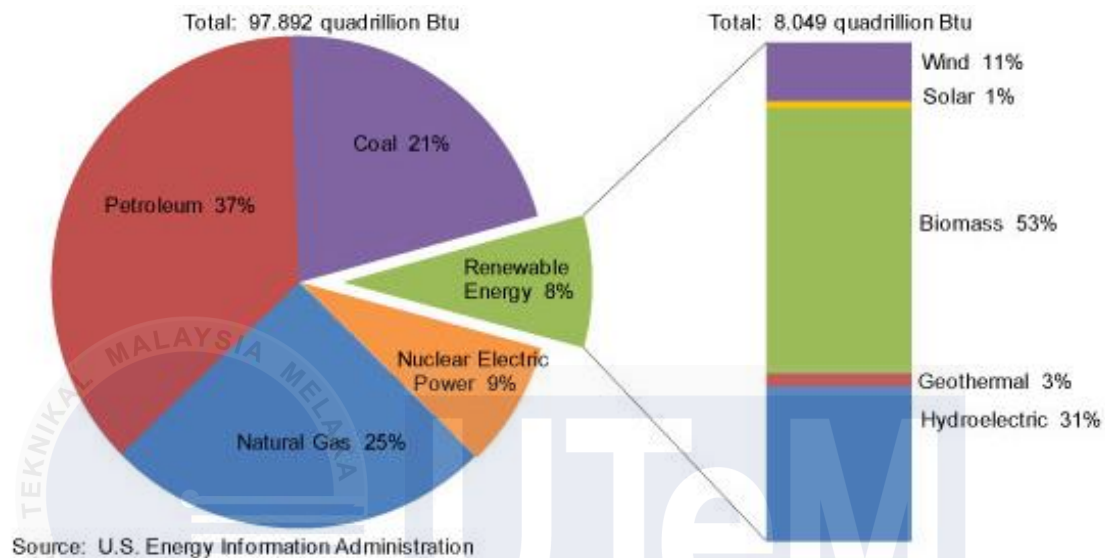


Figure 2.2 : Renewable energy's share of U.S. consumption in 2010[16]

As such, the reliance on fossil fuels poses significant challenges to achieving Sustainable Development Goal 7 (SDG 7), which aims to ensure access to affordable, reliable, sustainable, and modern energy for all[5]. By harnessing renewable sources such as solar, wind, hydro, biomass, and geothermal energy, nations can reduce their dependence on finite fossil fuels, mitigate climate impacts, improve energy access, and promote sustainable development on a global scale[18]. As technology advances and costs decrease, the adoption of renewable energy continues to grow, making it a crucial component of the global energy transition.

2.2.1 Solar Energy

Harnessing solar energy stands as a transformative force in the realm of renewable power. Solar energy referred to as radiant energy from the sun, represents a remarkable source of renewable power with extensive applications. This form of energy is harnessed through photovoltaic (PV) cells or solar thermal systems, converting sunlight into electricity or heat[11]. Solar power has gained widespread attention and adoption due to its eco-friendliness, reliability, and accessibility[19]. Additionally, advancements in solar technology, coupled with decreasing costs, have accelerated its integration into mainstream energy systems. Therefore, three types of solar panels exist, each with varying levels of efficiency and unique characteristics: Monocrystalline, Thin-film panels, and Polycrystalline[20].

2.2.1.1 Monocrystalline Solar Cell

Monocrystalline solar cell are renowned for their higher efficiency compare to other solar cell and durability in converting sunlight into electricity[21]. They are made from a 90% of crystalline silicon structure, resulting in a uniform appearance with a dark color[21]. This design allows monocrystalline panels to perform exceptionally well in low-light conditions and limited space installations[22]. Monocrystalline solar panels typically have an efficiency rate of around 20%, making them the highest compared to the other two types of solar cells[23]. Although they tend to be more expensive than other types of solar panels, their superior efficiency makes them a popular choice for residential and commercial solar systems where space is limited or aesthetics are a concern[24]. Monocrystalline panels are also known for their longevity, often lasting 25 years or more with minimal maintenance[25]. Figure 2.3 depicts a typical Monocrystalline solar cell commonly available in the market.



Figure 2.3 : Monocrystalline Solar Panel[24]

2.2.1.2 Polycrystalline Solar Cell

Polycrystalline solar panels, also known as multicrystalline panels, are made from silicon crystals that are melted together[26]. This manufacturing process is less costly than that of monocrystalline panels, making polycrystalline panels a more affordable option[27]. Polycrystalline solar panels generally achieve an efficiency rate of approximately 15% [23]. While they are generally less efficient than monocrystalline panels, polycrystalline panels still offer a reliable and effective solution for converting sunlight into electricity. Their distinctive blue hue and speckled appearance differentiate them visually from the uniform look of monocrystalline panels. Polycrystalline solar panels are a popular choice due to their long lifespan, often exceeding 25 years, making them a cost-effective and dependable option

for harnessing solar energy[28]. Figure 2.4 illustrates a standard Polycrystalline solar cell found in the market.



Figure 2.4 : Polycrystalline Solar Cell[24]

2.2.1.3 Thin-Film Solar Cell

Thin-film solar panels are made by depositing one or more layers of photovoltaic material onto a substrate, such as glass, plastic, or metal[29]. This manufacturing process allows for flexibility and a lightweight design, making thin-film panels versatile for various applications, including integration into buildings and portable solar solutions. However, thin-film panels generally have lower efficiency compared to monocrystalline and polycrystalline panels. Thin-film solar panels usually achieve an efficiency rate ranging from approximately 7% to 10% [23], meaning they require more surface area to produce the same

amount of electricity. Despite this, thin-film solar panels offer advantages in terms of cost and ease of installation, particularly in situations where weight and flexibility are crucial factors. Figure 2.5 showcases a Thin Film solar cell.



Figure 2.5 : Thin-Film Solar Cell[24]

2.3 Microcontroller

A microcontroller is a compact and integrated circuit that contains a processor core, memory, and input and output peripherals, all housed on a single chip[30]. These versatile devices are commonly used in embedded systems to control various functions and processes. Microcontrollers are programmable, allowing developers to write code and instructions to perform specific tasks. They come in different architectures and configurations, each suited for different applications and performance requirements[31]. Microcontrollers are widely used in electronics, automation, robotics, consumer electronics, automotive systems, and

many other fields where precise control and processing capabilities are essential. Their small size, low power consumption, and affordability make them indispensable components in modern technology, enabling the development of smart devices and systems across industries.

2.3.1 Arduino Uno

The Arduino Uno is a popular microcontroller board based on the ATmega328P microcontroller chip. As shown in Figure 2.6, It features digital input and output pins, analog inputs, a USB connection for programming and power supply, a reset button, and an ICSP (In-Circuit Serial Programming) header[32]. The board is designed to be user-friendly and accessible for beginners and hobbyists interested in electronics and programming. With an easy-to-use integrated development environment (IDE) and a vast community of users and resources, the Arduino Uno allows users to quickly prototype and develop projects ranging from simple LED blinking to more complex robotics and automation tasks.

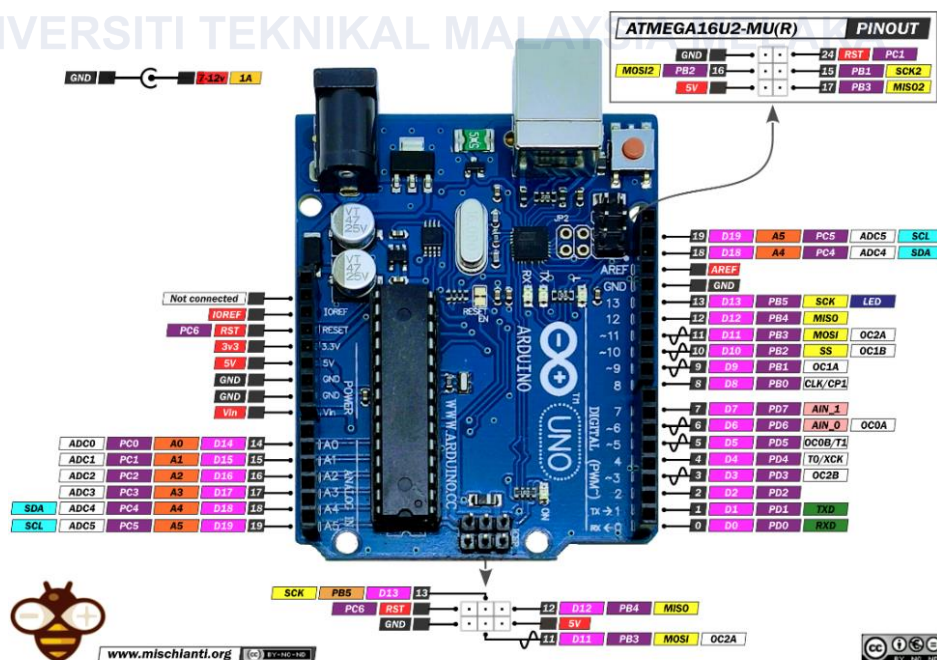


Figure 2.6 : Arduino Uno PinOut[33]

2.4 Storage System

A storage system for solar energy and batteries is a vital component in off-grid renewable energy setups. Figure 2.7 shown this system integrates solar panels for energy generation with batteries for energy storage, along with charge controllers to manage charging and discharging cycles[34]. The main purpose of this storage system is to capture excess solar energy during periods of high generation and store it in batteries for later use when sunlight is unavailable. This capability enables off-grid users to access reliable and sustainable energy, independent of traditional grid connections.

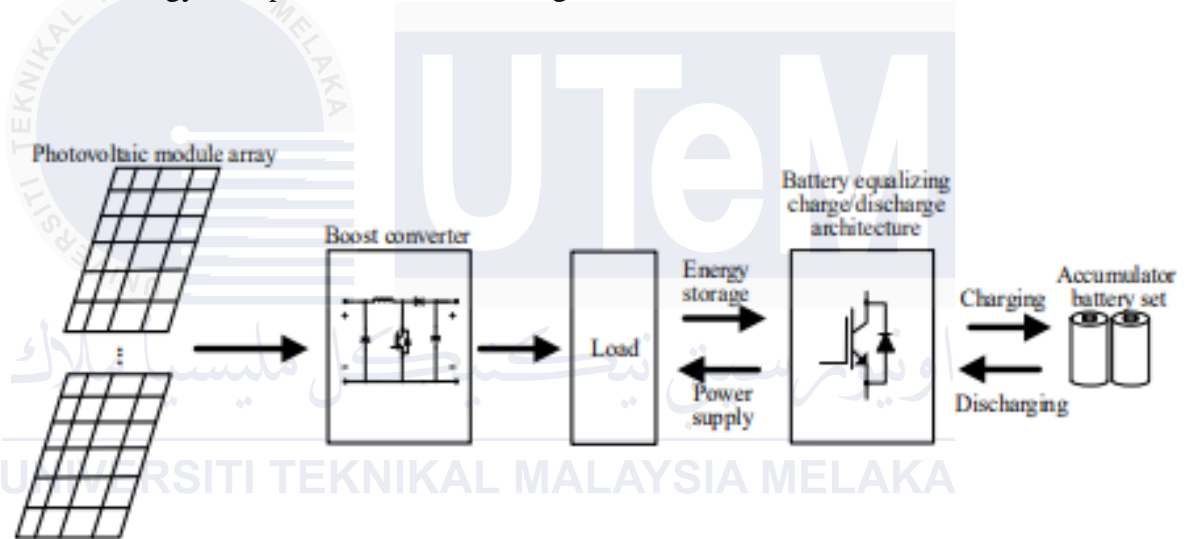


Figure 2.7 : Storage Battery System with Charge/Discharge Control[34]

2.4.1 Rechargeable Battery

Rechargeable batteries, also known as secondary batteries, are energy storage devices that can be recharged multiple times after discharging. These batteries are widely used in various electronic devices such as smartphones, laptops, electric vehicles, and renewable energy storage systems. Unlike disposable batteries (primary batteries), which are designed for single use and then discarded, rechargeable batteries are designed to be reused, reducing waste and environmental impact. They come in different chemistries, including

lithium-ion (Li-ion), nickel-metal hydride (NiMH), and lead-acid, each offering specific advantages and limitations in terms of energy density, lifespan, and charging capabilities. The table 2.1 illustrates the specifications of four different types of batteries.

Table 2.1 : Comparison 4 Type Common Rechargeable Batteries

Feature	Lithium-Ion[35]	Lithium-Polymer[36]	Lead Acid[37]	Nickel-Metal Hydride[38]
Weight (kg)	2.15	2	10	5.5
Specific Energy (Wh/kg)	150	150	40	65
Initial Cost (\$/kWh)	600	-	100	100
Typical State of Charge Window	80%	-	50%	-
Temperature Sensitivity	>45 °C	-	>25 °C	>45 °C
Efficiency	100% @ 20-hr-rate 99% @ 4-hr-rate 92% @ 1-hr-rate	-	100% @ 20-hr-rate 80% @ 4-hr-rate 60% @ 1-hr-rate	-
Voltage (increments)	3.7	3.7	2	1.2
Charging Temperature	0-45 °C	-	-	0-45 °C
Deep Cycle Life (times)	500	-	-	500

2.5 The Impact of pH Levels on Aquatic Ecosystems

The pH scale measures the acidity or alkalinity of a substance, ranging from 0 to 14, with 7 being neutral. Substances with a pH below 7 are acidic, while those above 7 are alkaline[39]. In aquatic environments, pH levels are crucial for the survival and well-being of aquatic animals. Alkaline conditions, with a pH above 8.5, can be harmful to aquatic organisms as they can disrupt metabolic processes and lead to imbalances in the ecosystem[40]. On the other hand, acidic conditions, with a pH below 6.5, can also be

detrimental, causing stress or even death in sensitive species[41]. Figure 2.8 illustrates the concentrations of hydrogen ions and hydroxide ions across the pH scale.

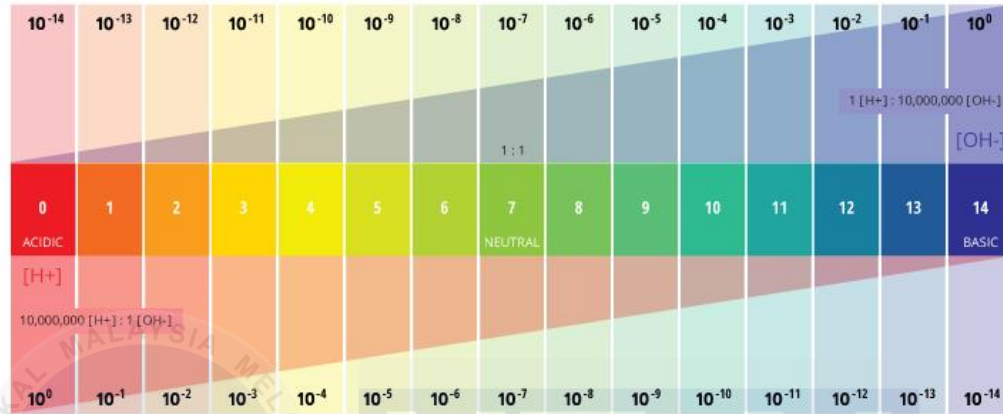


Figure 2.8 : Quantity Hydrogen Ion and Hydroxide Ion

2.6 Ph Sensor E-201-C

A pH sensor for Arduino is a critical tool in monitoring water quality and environmental conditions. It operates by detecting the acidity or alkalinity of a liquid solution, translating this information into a voltage signal. This voltage signal is then processed by the Arduino's analog-to-digital converter (ADC), allowing users to convert the voltage readings into pH values[42]. By calibrating the sensor with known pH solutions, the Arduino-based pH sensor can accurately measure and monitor pH levels in various applications, from hydroponics to aquariums, facilitating data-driven decision-making and control processes. Table 2.2 presents the pH values and corresponding voltages read by the E-201-C pH sensor, and Figure 2.9 displays the graph of this data.

Table 2.2 : pH Value and Voltage[43]

pH	Voltage(V)
0	3.74
1	3.57
2	3.39
3	3.22
4	3.04
5	2.87
6	2.69
7	2.52
8	2.34
9	2.16
10	1.99
11	1.81
12	1.64
13	1.46
14	1.29

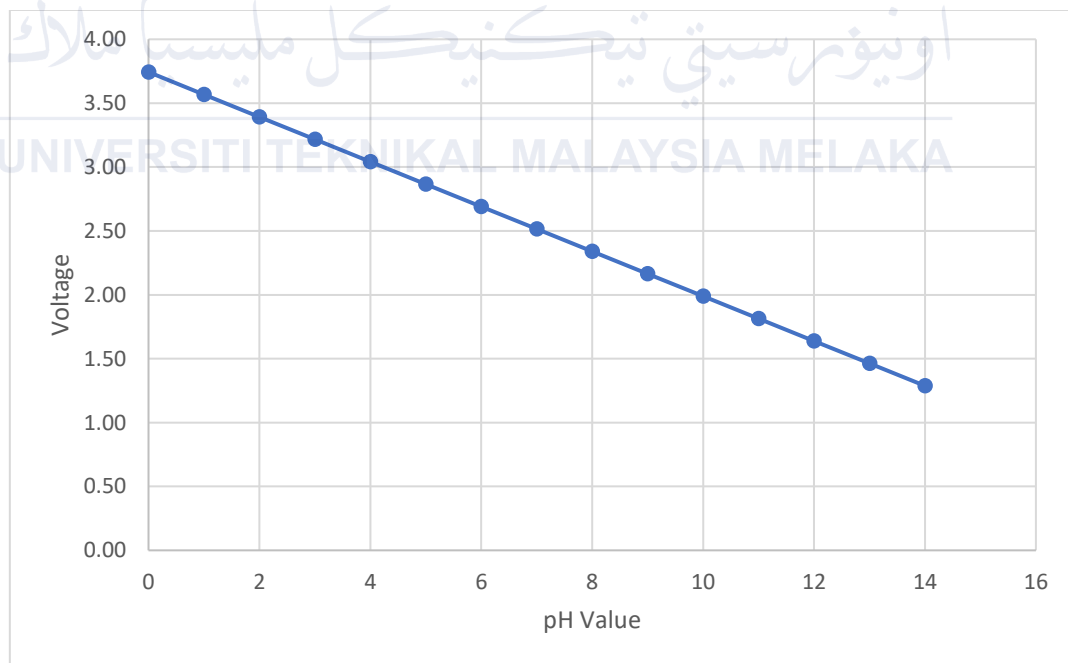


Figure 2.9 : Relationship Between pH Value and Voltage(V)

2.7 Summary on Development of Water Surface Cleaner

To ensure the success of the "Water Surface Cleaner Robot" project, thorough research into previous papers and studies related to similar projects is essential. In a study conducted by Siddhanna Janai[44], an ultrasonic distance measuring sensor was employed as part of a water surface cleaning robot. This sensor played a critical role in detecting obstacles and determining their distance from the watercraft. Additionally, the project integrated a smartphone and Bluetooth module to serve as a monitoring system for the boat, alongside a servo motor for control. A noteworthy aspect of this research was the utilization of the Blynk App as software to create a user-friendly application, enabling seamless control and monitoring of the robot's operations. These technological components were strategically combined to enhance the functionality, efficiency, and user experience of the water surface cleaning robot, showcasing the interdisciplinary nature of robotics and software integration in engineering projects. Figure 2.10 shown block diagram of the project.

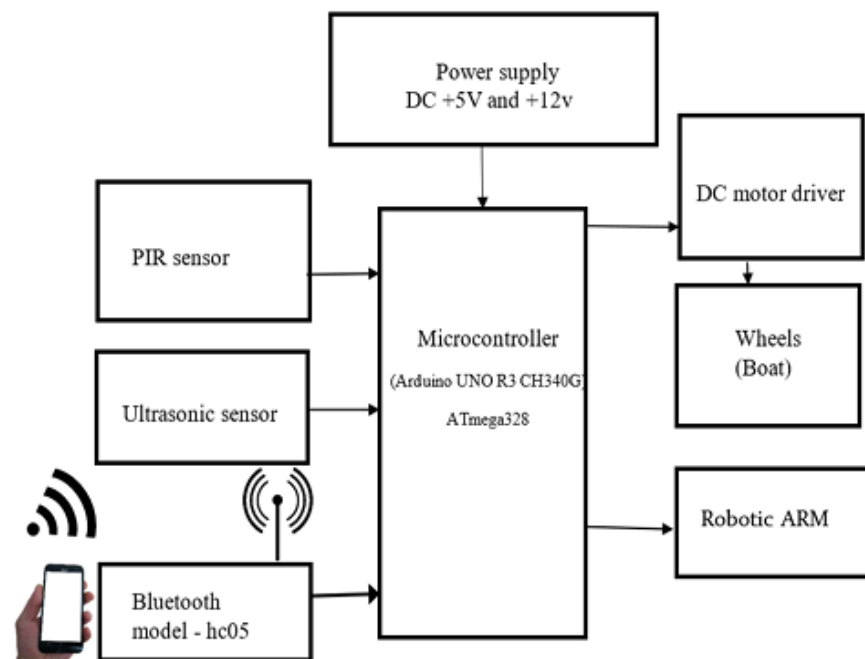


Figure 2.10 : Block Diagram of Siddhanna Project[44]

In a project led by Nurul Anis, the water surface cleaning robot was innovatively designed using polystyrene as the body material[45]. Polystyrene was selected for its lightweight properties, buoyancy, and durability, making it an ideal choice for aquatic applications. The robot featured motors mounted on its sides, providing efficient propulsion and manoeuvrability. To facilitate control and monitoring, the MIT App Inventor software was used to create a custom controller application. This application connected to the robot via the HC-05 Bluetooth module, enabling seamless wireless communication and user-friendly operation. This project highlights the integration of lightweight materials, efficient motor placement, and advanced software solutions to develop an effective and easily controllable water surface cleaning robot. Figure 2.11 depicts the fully developed robot, Such advancements contribute significantly to the field of environmental robotics, promoting innovative approaches to maintaining cleaner aquatic environments. . Figure 2.12 shown block diagram of the project.

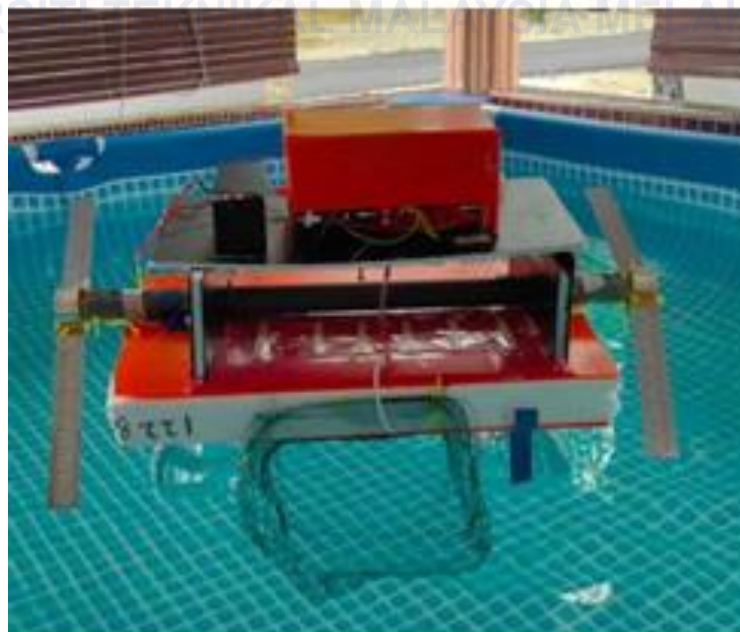


Figure 2.11 : Prototype of the Garbage Collector[45]

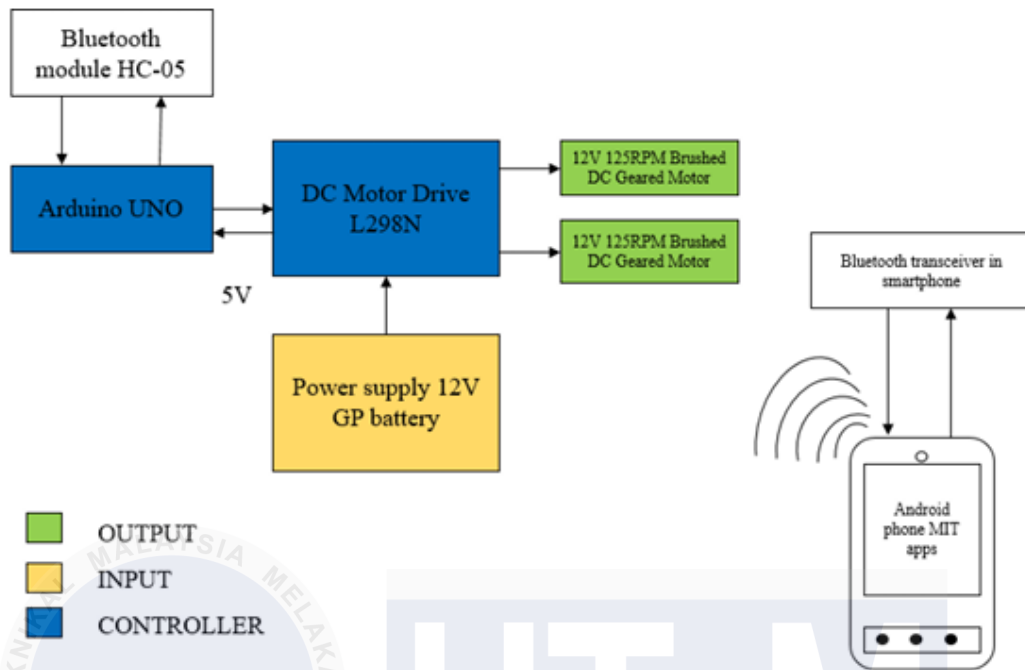


Figure 2.12 : Block Diagram of the System[45]

In another notable project by E. Rahmawati, a water surface cleaning robot was developed with a focus on efficient waste collection[46]. Figure 2.13 shows a prototype of the robot for the project. The robot, weighing approximately 8kg when empty and 28kg when loaded with garbage, utilized a manual control method for its operations. Control was facilitated through the integration of the Xbee Pro S2C module and the ZigBee BP24CZ7WIT-004, enabling robust wireless communication and remote operation. This project demonstrated the practical application of wireless technology in robotics, allowing for precise manual control and enhancing the robot's ability to navigate and clean water surfaces effectively. By addressing the challenges of waste management in aquatic environments, this research contributes to the advancement of environmental robotics and highlights the importance of integrating reliable communication technologies in the design and operation of cleaning robots.

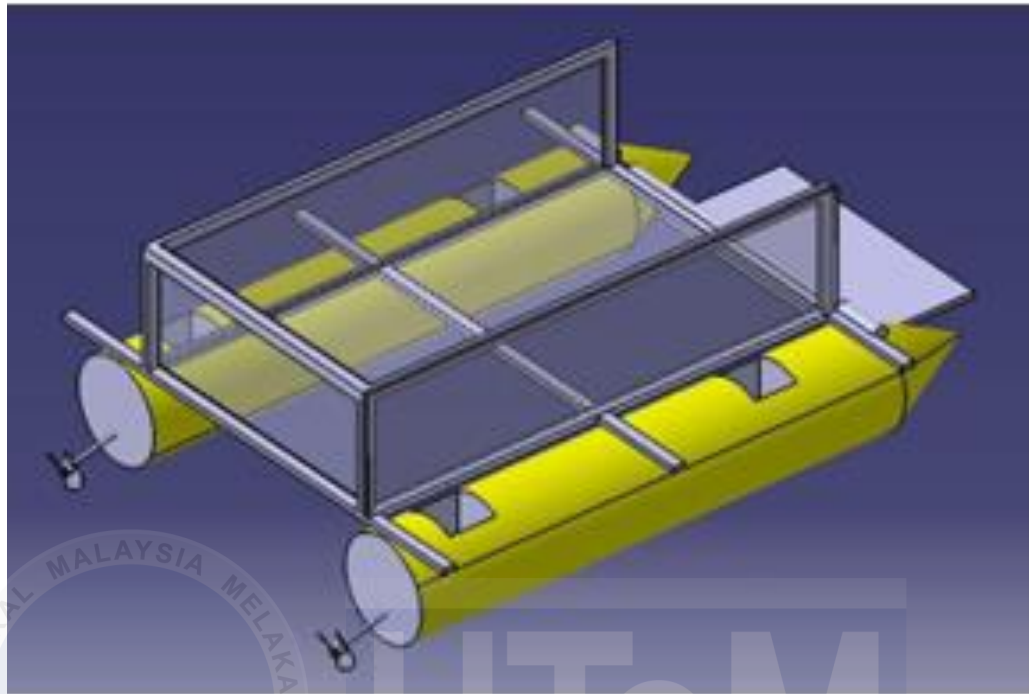


Figure 2.13 : Robot Prototype[46]

In a project led by Siti Farina, innovative materials and monitoring technologies were utilized to develop a water surface cleaning robot[47]. The robot's body was constructed using PVC pipes, chosen for their durability, buoyancy, and cost-effectiveness. This structural choice ensured the robot's resilience and effectiveness in aquatic environments. Additionally, the project incorporated an MIT PP inverter for monitoring and control, demonstrating the integration of advanced power management and monitoring systems. A pH sensor was also included to measure the water's pH levels, enabling the robot not only to

clean the surface but also to contribute to water quality assessment. Figure 2.14 provides an overall view depicting the positions of all components for this project.

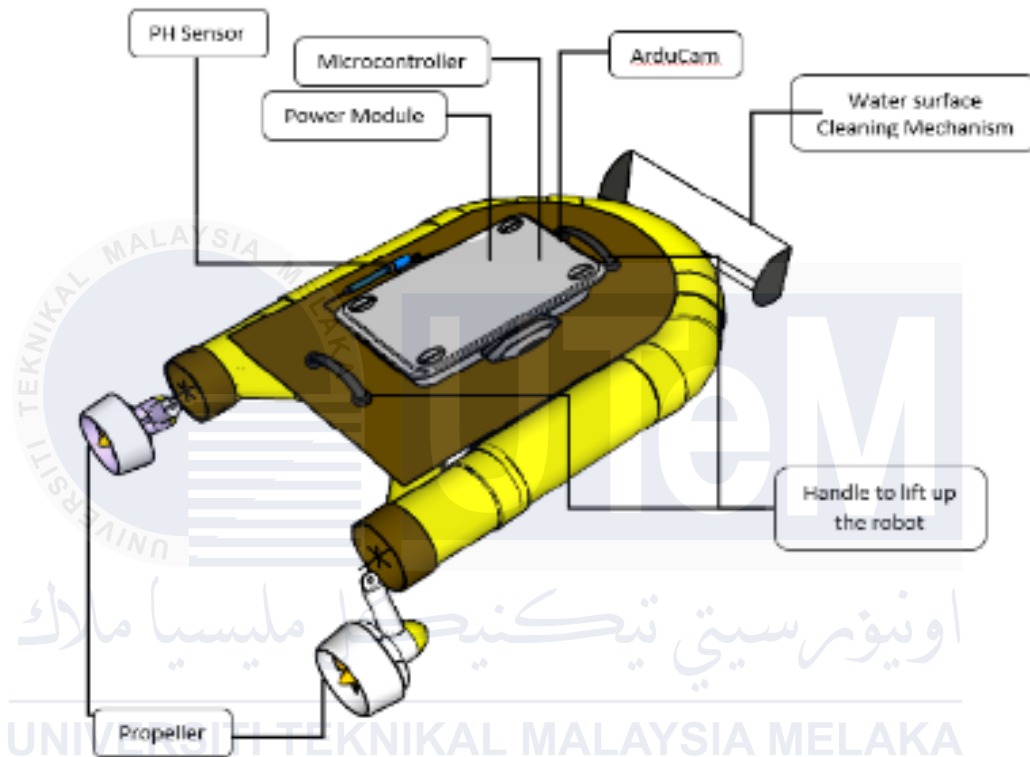


Figure 2.14 : Overall view of the positions of all components[47]

Based on the review of previous research and projects, it is evident that developing a water surface cleaning robot powered by solar energy is achievable. The successful integration of various technologies such as ultrasonic sensors for obstacle detection, wireless communication modules for control, and sustainable materials for construction demonstrates the feasibility of such a project. By incorporating solar panels and batteries, the robot can harness renewable energy, ensuring continuous and eco-friendly operation.

Table 2.3 : Summary on Development of Water Surface Cleaner

No.	Title	Authors	Application
1	Swachh Hasth - A Water Cleaning Robot[44]	Siddhanna Janai	Ultrasonic sensor - Detect Garbage Blynk App - Monitoring
2	Design and Development of a Solar-Powered Vacuum and Wet Cleaning Robot using Arduino UNO[48]	Dr. M. Vijayalakshmi Meghana Balu Pavani Chowla Pragna Sri Middela Harshini Bestha ⁵	Ground Surface Cleaning Ultrasonic sensor - Detect Garbage Solar And Battery - Generate and storage energy for robot
3	A Water Surface Cleaning Robot[46]	E Rahmawati I Sucahyo ¹ , A Asnawi M Faris ¹ , M A Taqwim D Mahendra	Weight of Robot - 28kg maximum with load Manual control Method - Xbee Pro S2C
4	Real-Time Monitoring System for an Aquatic Surface Cleaning Robot using MIT App Inventor[47]	Siti Farina Hidayah Zabidi Herdawatie Abdul Kadir Muhammad Danial ¹	Body Metarial - PVC Pipe PH Sensor - Measure pH water level MIT App Invertor - Monitoring
5	Development of Water Surface Mobile Garbage Collector Robot[45]	Ili Najaa Aimi Mohd Nordin Nurulaqilla Khamis Muhammad Rusydi Muhammad Razif	MIT App Inventor - Controller connect with Bluetooth Motor - Mounted on its sides

CHAPTER 3

METHODOLOGY

3.1 Introduction

When developing the water cleaning robot, the methodology comprises three key phases which identify all required components, simulating behaviour and performance, and designing in 2D and 3D. To enhance the clarity of the approach, a flowchart illustrating these phases and their interconnections is created. Initially, all necessary components such as motors, propellers, sensors, and microcontrollers are identified. Subsequently, by using Proteus 8, simulations are conducted to predict the robot's behaviour and performance under various conditions, optimizing the design and addressing potential issues early. Finally, detailed 2D and 3D designs are created using CAD software, generating schematics and realistic models to guide manufacturing and assembly processes. This comprehensive approach ensures the development of a reliable and efficient water cleaning robot.

3.2 Methodology

Objective 1 involves the design and simulation of electrical circuits that control the robot's movement, sensors, and other functionalities. Circuit simulation software is used to virtually test the circuits, allowing for error identification and rectification before physical construction begins. This step ensures that any potential issues are addressed early in the

design process. The process of the project can be illustrated as a block diagram in Figure 3.1.

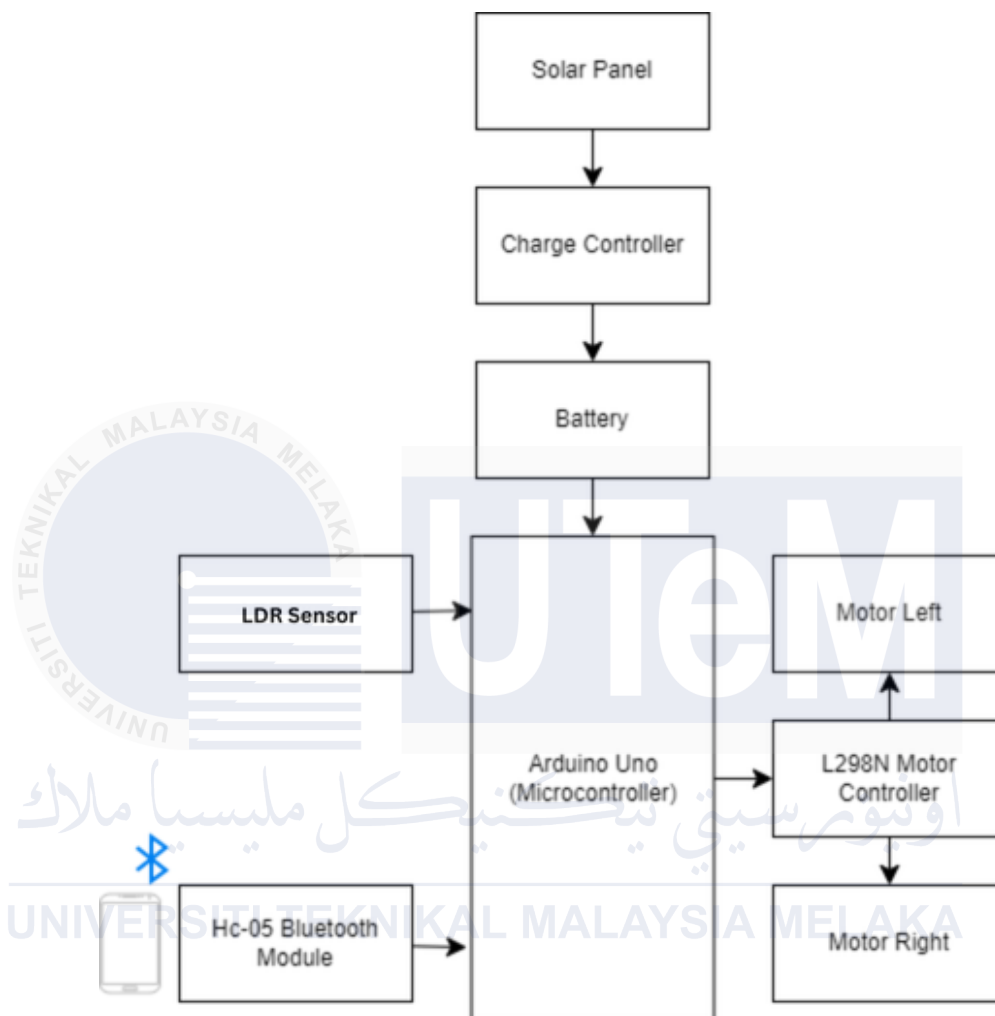


Figure 3.1 : Bolck Diagram Project

Objective 2, the physical components of the robot are assembled according to the blueprint. This includes integrating motors, sensors, a power source, a collection bin, and a frame to house all components. The focus is on building a robust and functional prototype that can be tested in real-world conditions.

Objective 3 entails rigorous testing to ensure the robot functions as intended. This phase evaluates the robot's mobility, debris collection efficiency, and stability in its aquatic environment. Data collected during testing is critical for identifying areas that need

improvement and refining the robot's design. This iterative process helps enhance the robot's performance and reliability. Figure 3.2 shown an overall project flowchart.

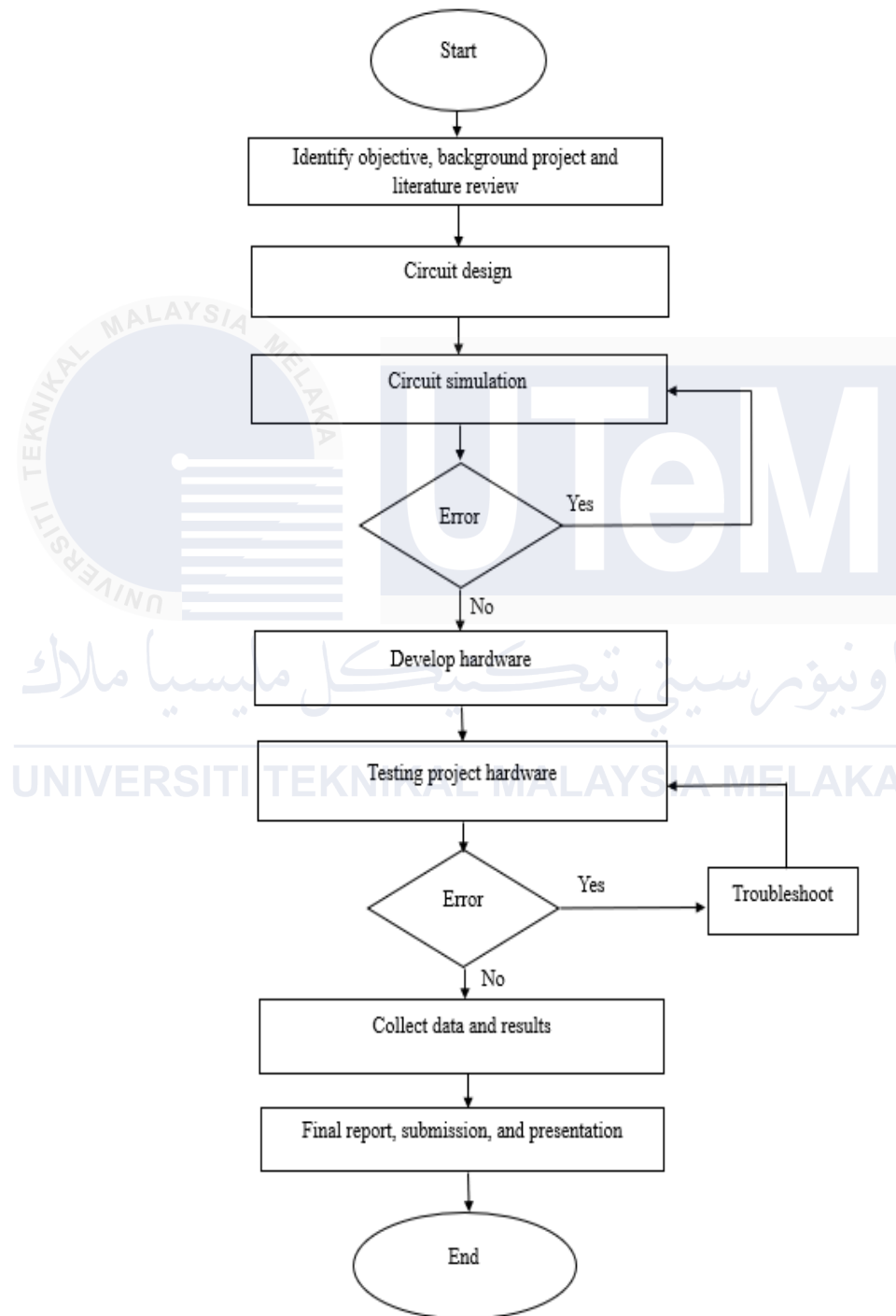


Figure 3.2 : Overall Project Flowchart

3.3 Simulation

In developing the water cleaning robot, the methodology unfolds through a series of steps represented as in Figure 3.3. To conduct simulations effectively, it's crucial to understand the flow of the project as depicted in the flowchart. This ensures that each step is followed in the correct sequence, starting from identifying necessary components and proceeding to simulation, design, and finally manufacturing and assembly. The flowchart serves as a visual guide that streamlines the development process, allowing for efficient optimization of the robot's behaviour and performance.

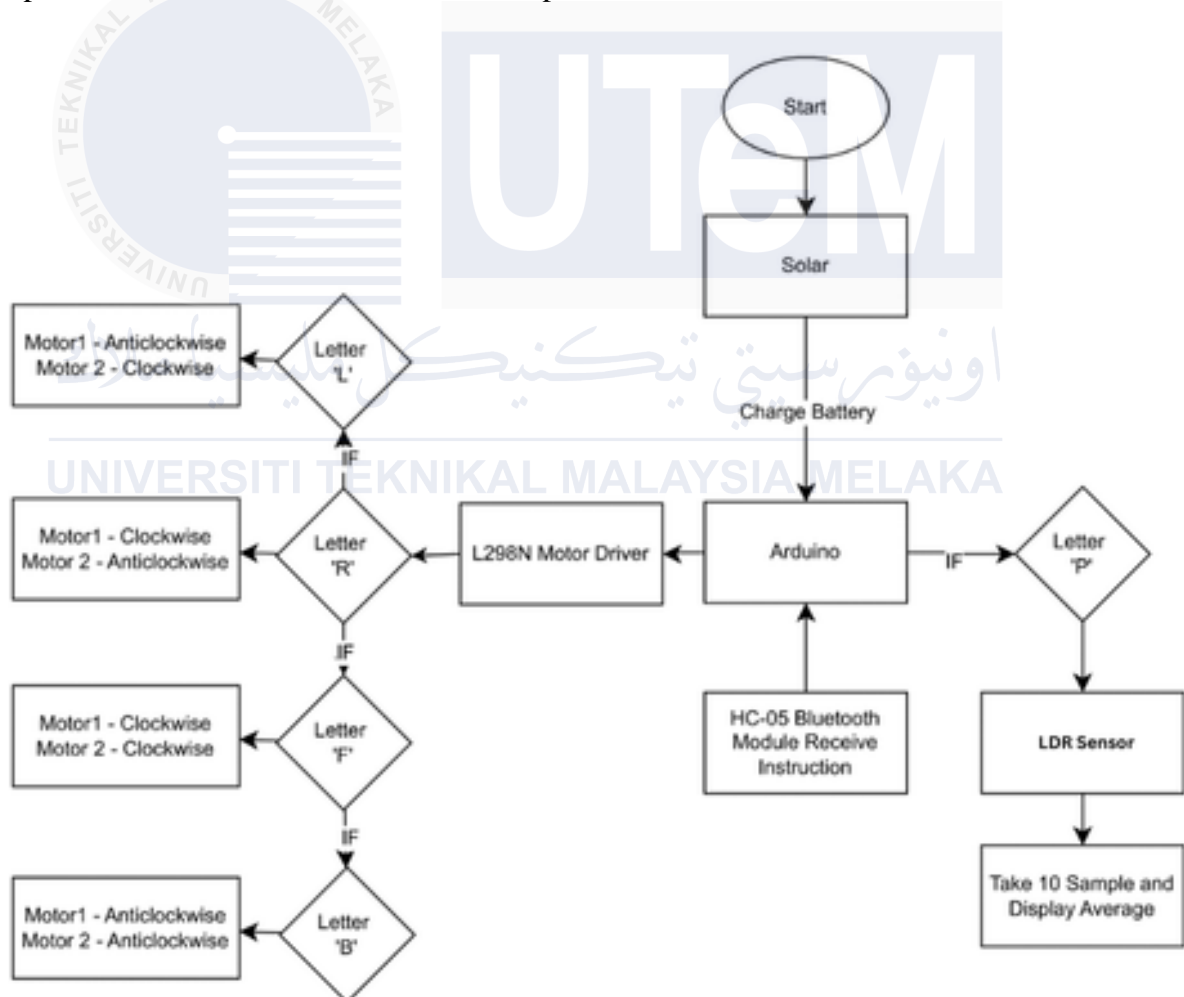


Figure 3.3 : Hardware Project Flowchart

3.3.1 Circuit Design And Simulation

The simulation journey begins with Proteus 8, a powerful Electronic Design Automation (EDA) software. Proteus 8 allows for meticulous design of the robot's electrical schematics, visual representations of components and their connections. Within this virtual environment, the project can simulate circuit behaviour, identifying and rectifying any potential issues before physically building the robot. Through simulation, the project guarantees proper power distribution, signal flow, and seamless communication between components, ensuring a robust electrical backbone for the robot.

3.3.2 Coding For Simulation

The project's core innovation emerges from integrating Arduino, a potent open-source electronics platform enabling code writing for physical circuit board control. Running simulations necessitates coding expertise. Utilizing Arduino, the project transforms user commands from the mobile app into precise instructions guiding the robot's motors, sensors, and cleaning mechanisms. Arduino's accessible coding language empowers hobbyists and professionals alike, fostering customization and adaptation of the robot's behaviour to cater to unique cleaning demands.

3.4 Application For Control Robot

Once the electrical blueprint is solidified, the project turns its attention to user control and robot intelligence. In this stage, MIT App Inventor steps onto the stage as a user-friendly, visual programming tool for developing a mobile application to control the robot. Imagine a user interface that empowers effortless commands for the robot's movements, activation of

its cleaning mechanisms, and potentially even monitoring sensor data. Figure 3.4 shown a flowchart for application input and output.

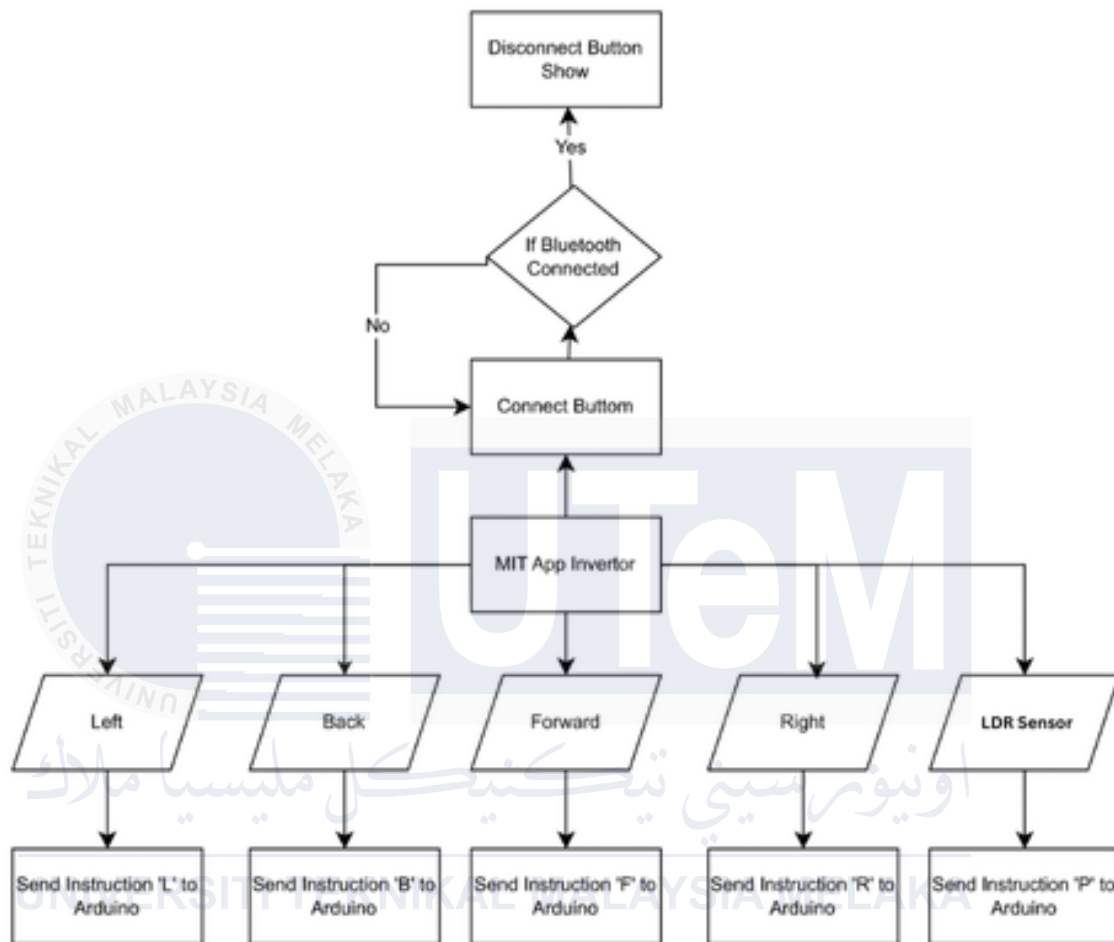


Figure 3.4 : Application Flowchart

3.5 2D and 3D Design

Finally, the project will leverage the precision of AutoCAD, a powerful 2D and 3D design software. AutoCAD will be instrumental in creating detailed technical drawings of the robot. Imagine a comprehensive set of 2D schematics that clearly illustrate the robot's physical layout, including the exact placement and dimensions of each component. These schematics will serve as a blueprint for construction, ensuring a smooth and accurate

assembly process. Furthermore, AutoCAD allows for the creation of 3D models of the robot. These models provide invaluable benefits, allowing for visualization of the robot's final design from any angle, identification of potential assembly clashes or design flaws before construction begins.

3.6 Experiment Setup

This project proposes the development of a water cleaning robot, utilizing a unique blend of software tools, Arduino for coding, and physical experimentation. This comprehensive approach ensures the robot's functionality, user-friendliness, and efficient operation while thoroughly evaluating its effectiveness in both simulated and real-world challenges.

By strategically combining Proteus 8, MIT App Inventor, AutoCAD, and the power of Arduino for coding, this project adopts a holistic approach. It not only designs and simulates robust electrical circuits but also creates a user-friendly mobile app for control and leverages the power of 3D visualization for accurate and efficient construction. The integration of Arduino adds a level of customization and real-world interaction, enhancing the robot's capabilities.

Physical experiments are conducted alongside software simulations to test the robot's performance in realistic water cleaning scenarios. This hands-on testing ensures that the robot is not only functional in theory but also practical and reliable in real-life applications. This multi-software methodology, combined with Arduino and rigorous physical

experimentation, paves the way for the development of a truly functional and adaptable water cleaning robot—a valuable tool in our fight for cleaner waterways.

3.6.1 PVC Pipe Sizing : Buoyancy Test

The purpose of this experiment is to determine the submerged limit of a 2.5-inch PVC pipe to assess its suitability for use in a floating robot. Understanding the submerged limit is crucial for selecting the optimal material for constructing a floating robot, as it influences the robot's ability to remain afloat under varying conditions and loads. By testing the pipe with different weights, this experiment aims to identify the maximum weight the pipe can support before submersion.

To conduct the experiment, as shown as in Figure 3.5, a 2.5-inch PVC pipe was selected, cut to 50cm, and sealed at both ends to prevent water from entering. The pipe was submerged in a water, and the submersion depth was measured under three different weight conditions, as shown as in Figure 3.6. Each test was repeated three times to ensure accuracy and consistency. Weights were securely attached to the pipe before measuring the depth of submersion.



Figure 3.5: Pipe Setup



(a)

(b)

Figure 3.6 : Floating test with Load

During the experiment, the depth of submersion for the pipe under each weight condition was carefully recorded. This data was organized into a table for analysis. The recorded values included the submersion depth for the 2.5-inch pipe under all three weight conditions. These measurements were analysed to determine the submerged limit of the pipe and its suitability for the floating robot design.

3.6.2 Robot Cleaning Movement and Speed

The purpose of this experiment is to measure the time taken by the robot to travel a distance of 3 meters under three load conditions: without load, with a 3 kg load, and with a 6 kg load. This experiment helps evaluate how additional weight affects the robot's speed and performance, providing insights into its efficiency and operational limits under different

load conditions. Figure 3.7 illustrates the experimental setup, with each brick marking a 1-meter distance.



Figure 3.7 : Distance Setup

To conduct the experiment, the robot was placed on a flat, level surface to ensure consistent movement. A 3-meter track was marked, and a stopwatch was used to measure the time taken for the robot to complete the distance. The robot was first tested without any load, and the time was recorded. Next, a 3 kg load was securely attached to the robot as in

Figure 3.8, and the process was repeated. Finally, a 6 kg load was added, and the robot was tested again. Each test was performed three times to ensure accurate and reliable results.

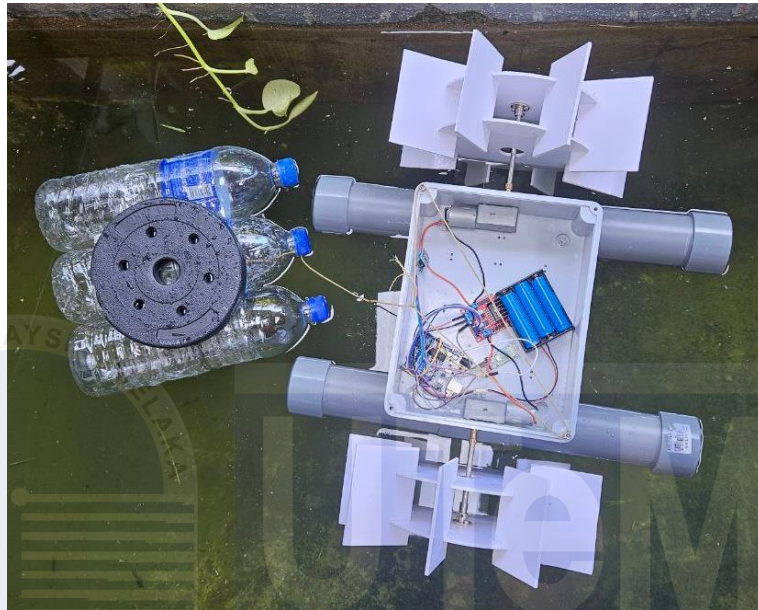


Figure 3.8 : Robot Cleaner with Load

The time taken for the robot to travel 3 meters under each load condition was recorded for every trial. The data was averaged to account for any variations between trials. The results were then analysed to determine how the robot's speed changes as the load increases, providing valuable information for optimizing the robot's design for practical applications.

3.6.3 HC05 Bluetooth Signal Limit Distance

The objective of this experiment is to determine the maximum effective distance of the HC-05 Bluetooth module's signal. This test is essential for understanding the

communication range limitations of the module, which is critical for designing systems that rely on Bluetooth connectivity.

To conduct the experiment, as illustrated in Figure 3.9, the HC-05 Bluetooth module was paired with a smartphone using a Bluetooth communication application. A buzzer was used as the output to indicate whether the module was receiving a signal. The module and buzzer setup was placed in an open area to minimize interference from walls or other obstructions. A measuring tape was used to mark distances at 1-meter intervals.

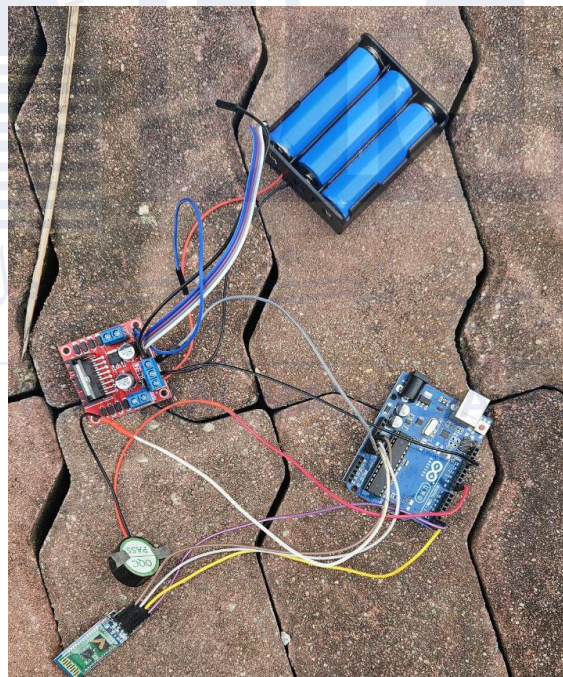


Figure 3.9 : Bluetooth Distance Setup

Starting at 1 meter, a connection test was performed by sending a signal from the smartphone to activate the buzzer. If the buzzer turned on, it indicated that the Bluetooth module was still receiving the signal. The distance was then incrementally increased by 1

meter, and the process was repeated until the buzzer failed to activate, signalling a loss of connection. Each test was repeated three times for consistency.

The maximum distance at which the buzzer activated reliably was recorded. For each trial, the distance at which the buzzer failed to activate or produced intermittent behaviour was also noted. The results were analysed to identify the HC-05 module's effective communication range, providing valuable data for its application in wireless systems.

3.6.4 Effect of Sun brightness, temperature and Humidity toward solar efficiency

The purpose of this experiment is to analyse how environmental factors sun brightness, temperature, and humidity affect the efficiency of a solar panel by measuring its output voltage under different conditions. This experiment is crucial for understanding how real-world environmental variables influence the performance of solar energy systems.

The solar panel was placed in an open area with maximum exposure to sunlight. A digital multimeter was connected to the panel to measure its output voltage. Environmental conditions were monitored using sensors: a DHT11 sensor was used to measure temperature and humidity, while an LDR (Light Dependent Resistor) sensor was employed to measure sunlight brightness.

Data collection was performed at three specific times of the day, 8:00 AM (morning), 1:00 PM (noon), and 6:00 PM (evening) to capture varying environmental conditions. This

schedule was selected to observe the effects of changing sunlight intensity, temperature, and humidity levels on the solar panel's output. The experimental setup is shown in Figure 3.10.

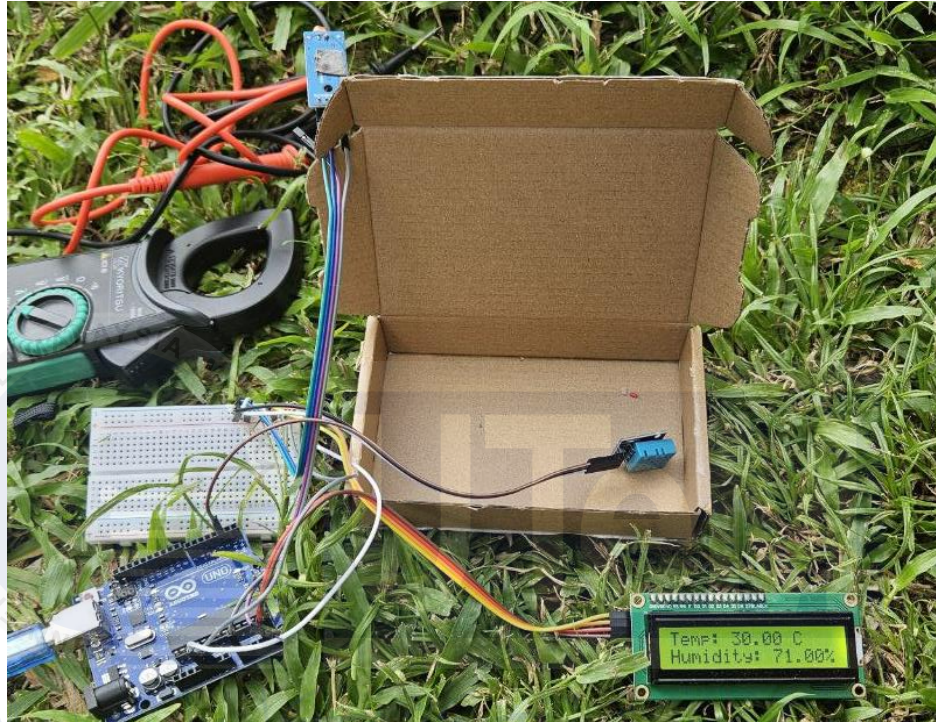


Figure 3.10 : DHT11 and LDR sensor Setup

The output voltage of the solar panel was recorded alongside the corresponding sun brightness, temperature, and humidity values during each measurement. These data points were compiled into a table for further analysis. The relationship between the environmental variables and the solar panel's output voltage was then evaluated to determine how each factor influences the solar panel's efficiency under different conditions.

3.6.5 Motor rotation speed

The objective of this experiment is to measure the rotational speed of a motor using an IR sensor and a handmade encoder. This experiment is crucial for determining the motor's

performance, particularly in applications where precise rotational speed measurement is required.

To conduct the experiment, as shown in Figure 3.11, a DC motor was powered with a fixed 12V input and set up on a test rig. A handmade encoder disk, designed with evenly spaced patterns, was attached to the motor shaft. The IR sensor was positioned close to the encoder disk to detect the changes in reflection as the motor rotated. Each pattern on the encoder disk corresponded to one rotation, and the IR sensor generated a pulse for every rotation detected.

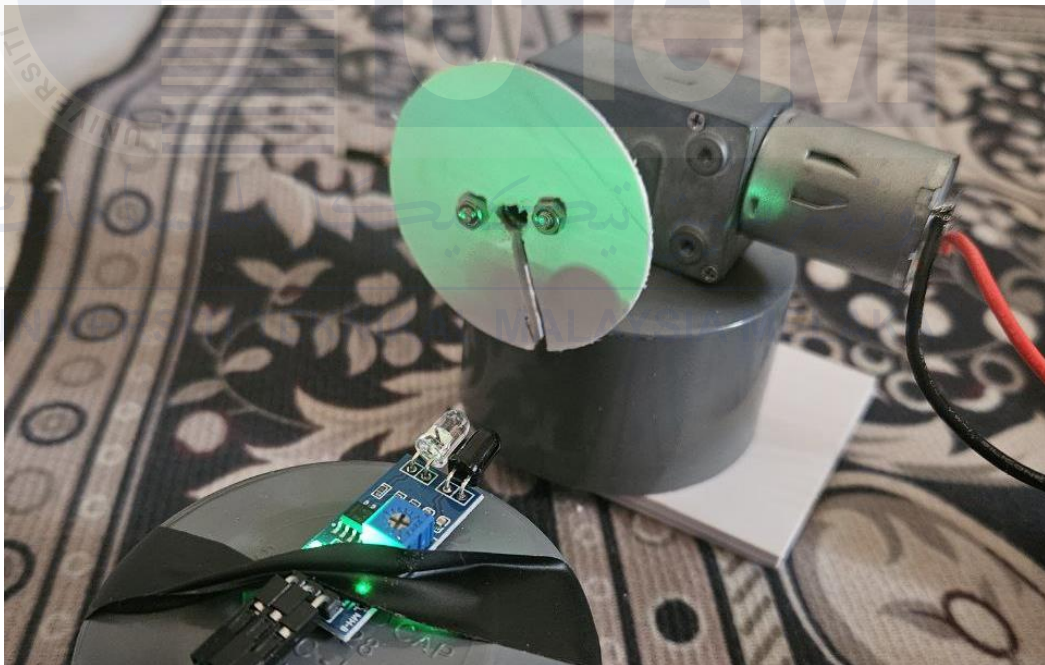


Figure 3.11 : IR Sensor and DC motor Setup

The motor was powered at 12V and allowed to run continuously for one minute. During this time, the IR sensor counted the pulses generated by the encoder. These pulses were recorded using a microcontroller or digital counter. Since each pulse represented one

full rotation, the total pulse count over the one-minute period directly corresponded to the number of rotations completed by the motor.

3.7 List of Hardware

3.7.1 Arduino Uno

The Arduino Uno, as shown in figure 3.12, will be used as the primary microcontroller for this project due to its flexibility, which is advantageous for future expansions and modifications. Its user-friendly interface and extensive library support make it an ideal choice for both beginners and experienced developers.



Figure 3.12 : Arduino Uno

3.7.2 L298N Motor Driver

The L298N motor driver is an ideal choice for this project due to its capability to control two motors simultaneously. This feature allows for efficient and synchronized operation of the robot's propulsion system. Additionally, the L298N motor driver can supply

12V separately to each motor, ensuring adequate power for robust and reliable performance.

Figure 3.13 illustrates the L298N motor driver, which is available in the market.

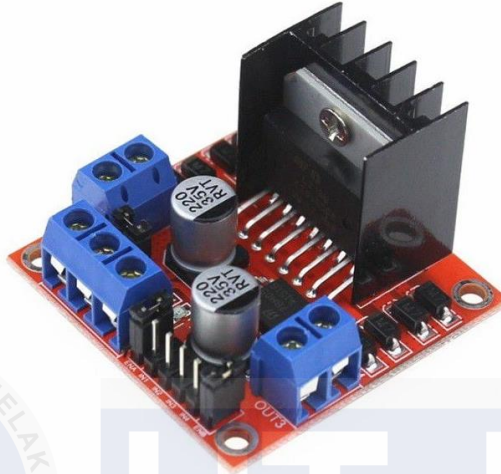


Figure 3.13 : L298N Motor Driver

3.7.3 Hc-05 Bluetooth Module

The HC-05 Bluetooth module is utilized in this project to enable wireless communication, which is essential for remote control capabilities. By incorporating the HC-05, the project can leverage Bluetooth technology to connect the Arduino microcontroller with a custom-developed mobile app. This app will serve as the controller, allowing users to send commands and receive feedback from the robot seamlessly. Figure 3.14 depicts the HC-05 Bluetooth module, commonly available in the market.

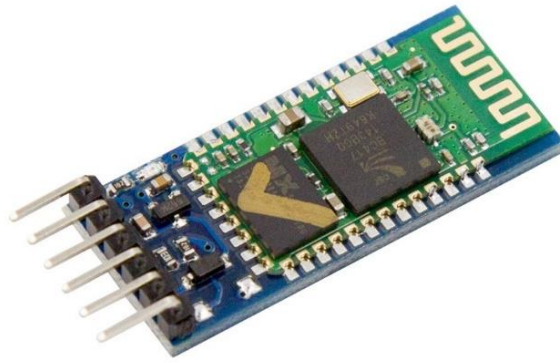


Figure 3.14 : Hc-05 Bluetooth Module

3.7.4 DC Motor

The use of DC motors in this project is essential for enabling the movement of the robot. DC motors are highly effective due to their ability to rotate both clockwise and anticlockwise, providing versatile and precise control over the robot's movements. This bidirectional capability allows the robot to navigate efficiently in various directions, enhancing its manoeuvrability and effectiveness in cleaning tasks. Figure 3.15 shows an example of a DC motor available in the market.



Figure 3.15 : Dc Motor

3.7.5 12V Solar Panel

The decision to incorporate a monocrystalline solar panel in this project stems from the need for a compact and space-limited power source. The small size as shown in Figure 3.16, the solar panel makes it ideal for integration onto the water cleaning robot, where space is a premium. Additionally, the capacity is sufficient to charge a 12V battery, providing a renewable and environmentally friendly power solution for prolonged operation without relying on external power sources.

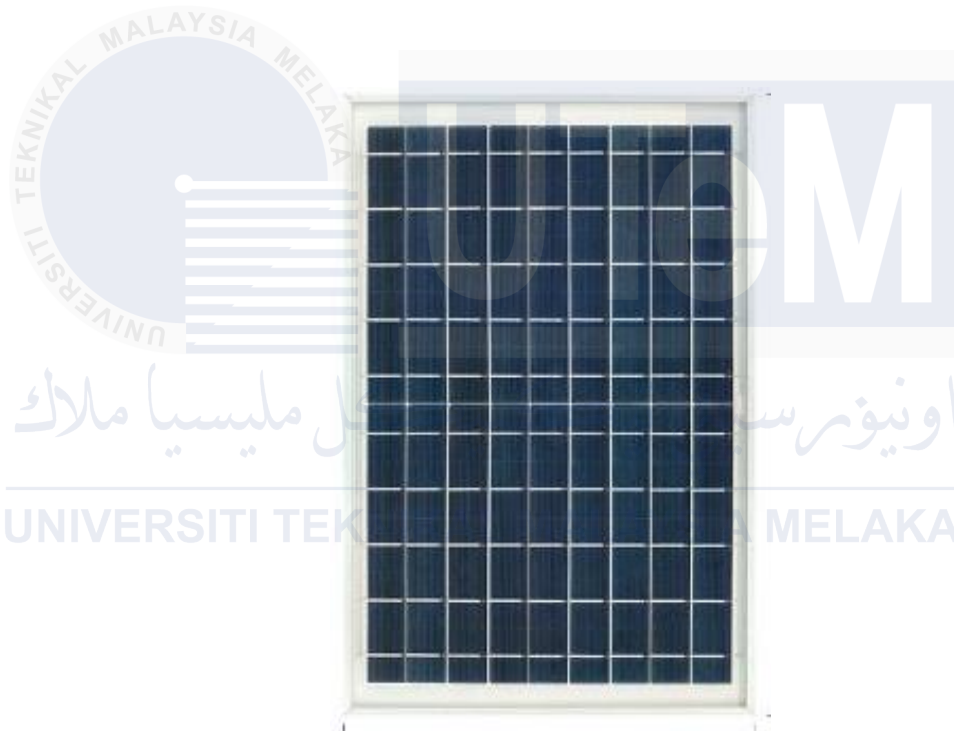


Figure 3.16 : Solar Monocrystalline

3.7.6 Charge Controller

The inclusion of a charge controller in this project is essential for effectively managing the charging and discharging processes of the battery. A charge controller ensures that the battery receives an optimal charge without overcharging, which can damage the battery over time. Figure 3.17 illustrates a charge controller commonly available in the

market. Additionally, the charge controller regulates the discharge of the battery, preventing excessive discharge that could lead to reduced battery lifespan.



Figure 3.17 : Charge Controller

3.7.7 Lithium Ion Battery

Figure 3.18 depicts a Lithium Ion Battery. The decision to utilize a lithium-ion battery in this project is driven by its compact and lightweight nature, making it an ideal power source for the water cleaning robot. The small size and low weight of lithium-ion batteries allow for easy integration without adding significant bulk to the robot's design.



Figure 3.18 : Lithium Ion Battery

3.8 Summary

The methodology for developing a water cleaning robot encompasses several key phases that are interlinked for a cohesive and efficient workflow. Initially, the process begins with identifying all necessary components crucial to the robot's functionality, followed by designing and simulating electrical circuits to ensure optimal performance. This simulation phase allows for the early identification and rectification of any potential issues, laying a strong foundation for the physical assembly of the robot's components. Subsequently, the robot is physically assembled according to the finalized design, focusing on robustness and functionality. The fourth phase involves rigorous testing in real-world conditions to evaluate the robot's mobility, cleaning efficiency, and overall performance, providing valuable data for further refinement. Finally, the entire development process is comprehensively documented, detailing objectives, methodologies, results, and conclusions. This structured approach, combined with the integration of software tools like Proteus 8, MIT App Inventor, AutoCAD, and Arduino, ensures a systematic and effective development journey towards creating a reliable and efficient water cleaning robot.

CHAPTER 4

PRELIMINARY RESULTS AND DISCUSSIONS

4.1 Introduction

This chapter provides an in-depth exploration of the progress and outcomes of the Water Cleaning Robot project, comprehensively detailing the entire system and discussing various obstacles and advancements encountered during development. It elucidates the expected outcomes and limitations inherent in the system's design and implementation, delves into the testing and analysis of the system's application, highlights the output results, and examines the influence of varying input parameters. Through rigorous testing and analysis, this chapter aims to provide valuable insights into the performance and efficacy of the innovative water cleaning robot, thereby contributing to a deeper understanding of its practical implications and potential for real-world deployment.

4.2 Results and Analysis

Completion of the simulation phase has yielded preliminary results that provide valuable insights into the performance and feasibility of the water cleaning robot. Simulations conducted using Proteus 8 for circuit design, MIT App Inventor for control interface development, and AutoCAD for 2D and 3D modelling have enabled predictions of the robot's behaviour and early identification of potential issues before physical prototyping. The analysis is divided into four key components: the HC-05 Bluetooth module, the motor system, the solar and storage system. Each part has been meticulously simulated to ensure seamless integration and optimal performance in the final design.

4.2.1 Complete Circuit

The fully completed circuit simulation is depicted in Figure 4.1, showcasing the comprehensive integration of components. The process initiates with the HC-05 Bluetooth module establishing a Bluetooth connection, making it available for the app controller to connect with the Arduino microcontroller seamlessly. Once the connection is established, the app can send instructions to the Arduino based on the user's interactions with the screen. This interaction enables precise control over the water cleaning robot's movements and functionalities, enhancing user experience and operational efficiency.

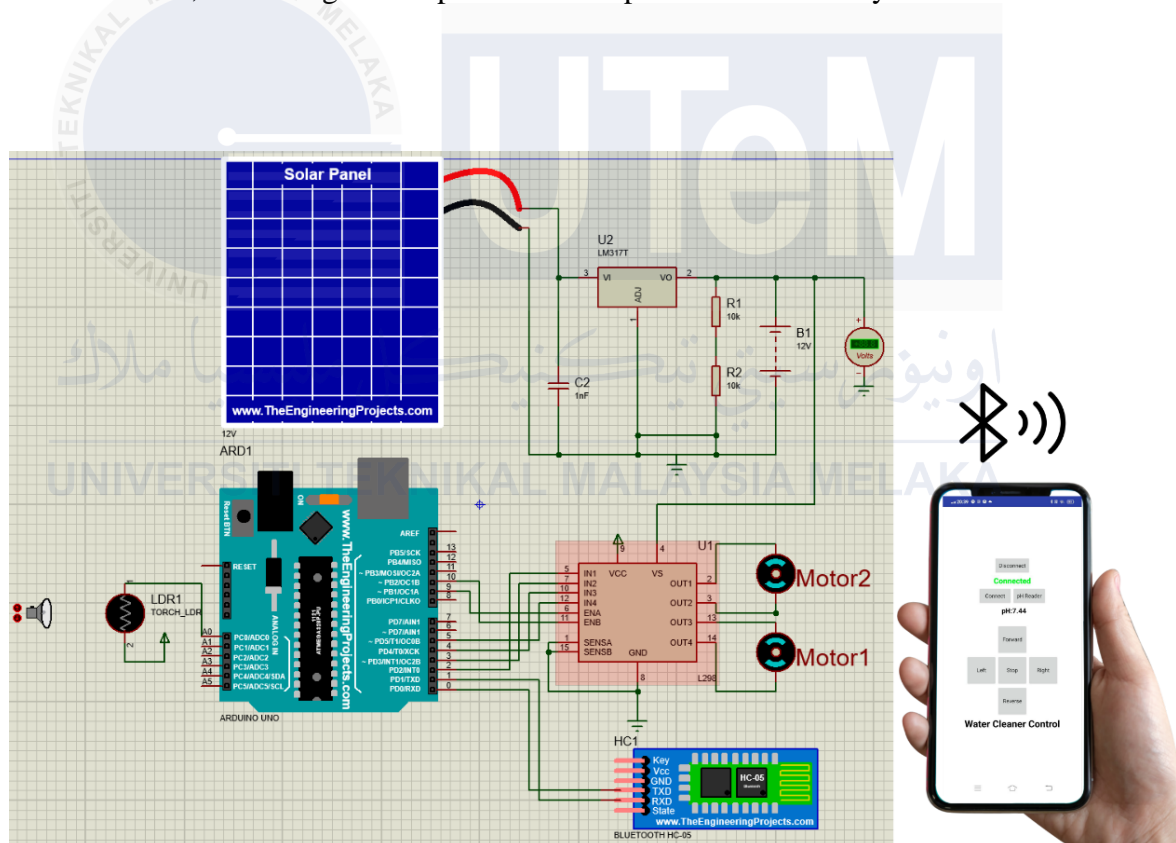


Figure 4.1 : Full Complete Circuit

4.2.2 Complete Application

The mobile app designed for this project features several key functionalities for seamless control and monitoring of the water cleaning robot. Firstly, the app includes a "Connect" button, which, initiates the Bluetooth connection process. Once the connection is established successfully, the "Disconnect" button becomes visible, allowing users to disconnect the Bluetooth connection as needed.

The app interface incorporates intuitive control buttons for precise navigation of the robot, as shown in Figure 4.2, enabling users to command forward, backward, left, and right motions during cleaning operations. Additionally, The app integrates an LDR sensor functionality that displays real-time feedback on sunlight intensity, aiding users in optimizing solar efficiency and maintaining sustainable energy conditions.

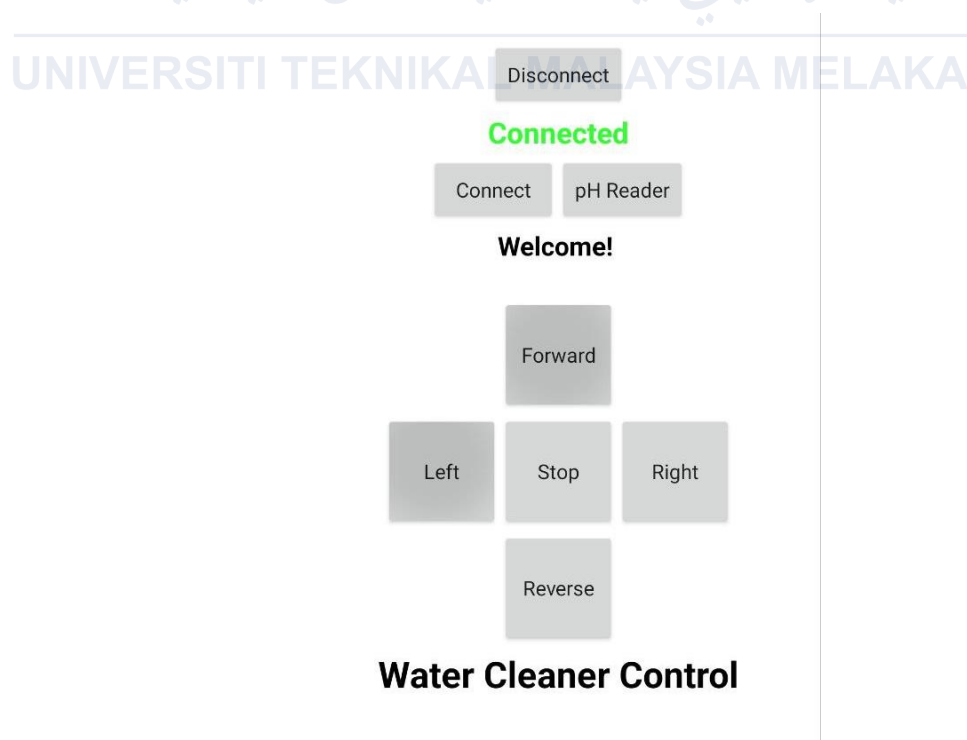


Figure 4.2 : Complete Application

4.2.3 Complete 2D and 3D Design

The design of the robot incorporates specific features for functional efficiency and protection of its components. Firstly, the position of the fan blade motor is strategically placed to avoid contact with water, ensuring durability and consistent performance. Secondly, the robot has a flat top design, which allows the solar panel to stay flat and secure on top, optimizing solar energy absorption. Lastly, a central box is included to house the electronic components, safeguarding them from water exposure and potential damage. Figure 4.3 is a 2D design prototype, while Figure 4.4 is a 3D prototype of the project.

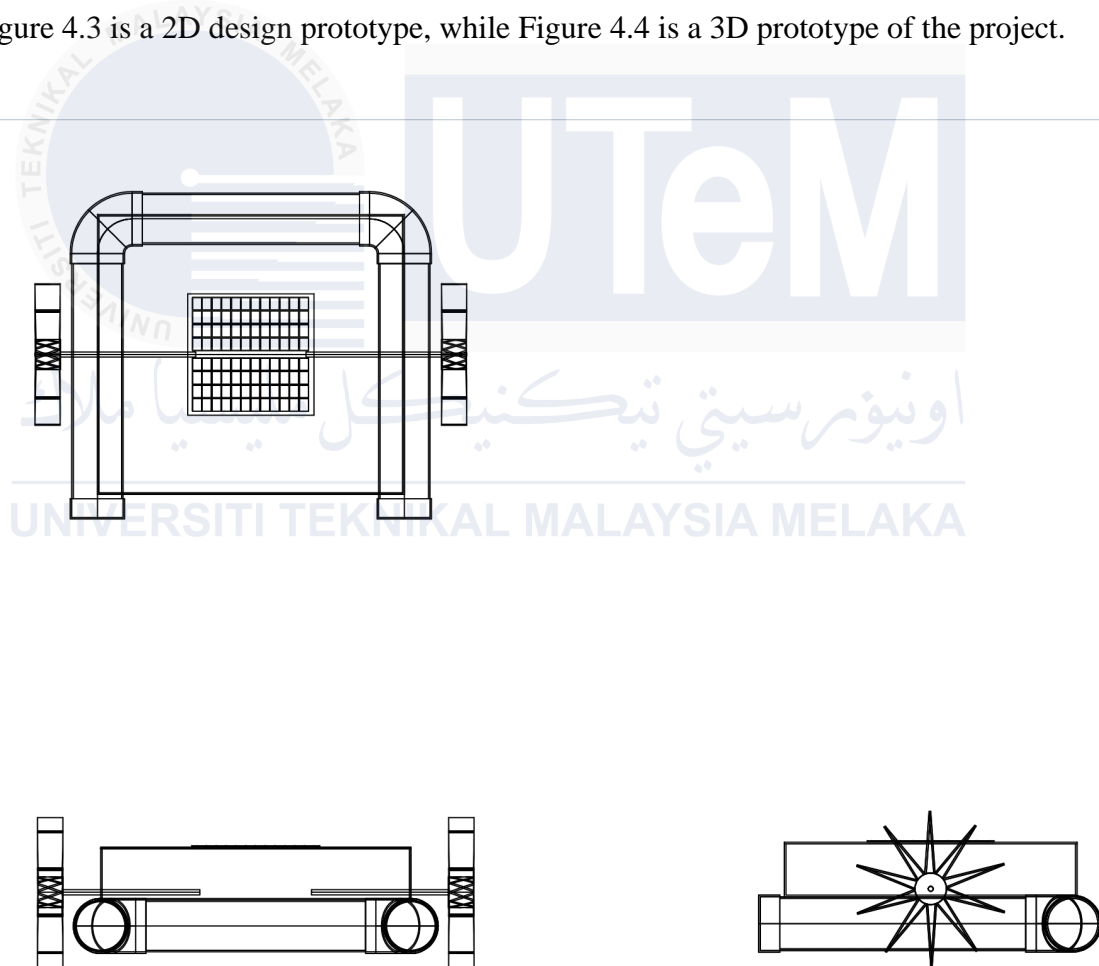


Figure 4.3 : 2D Project Design

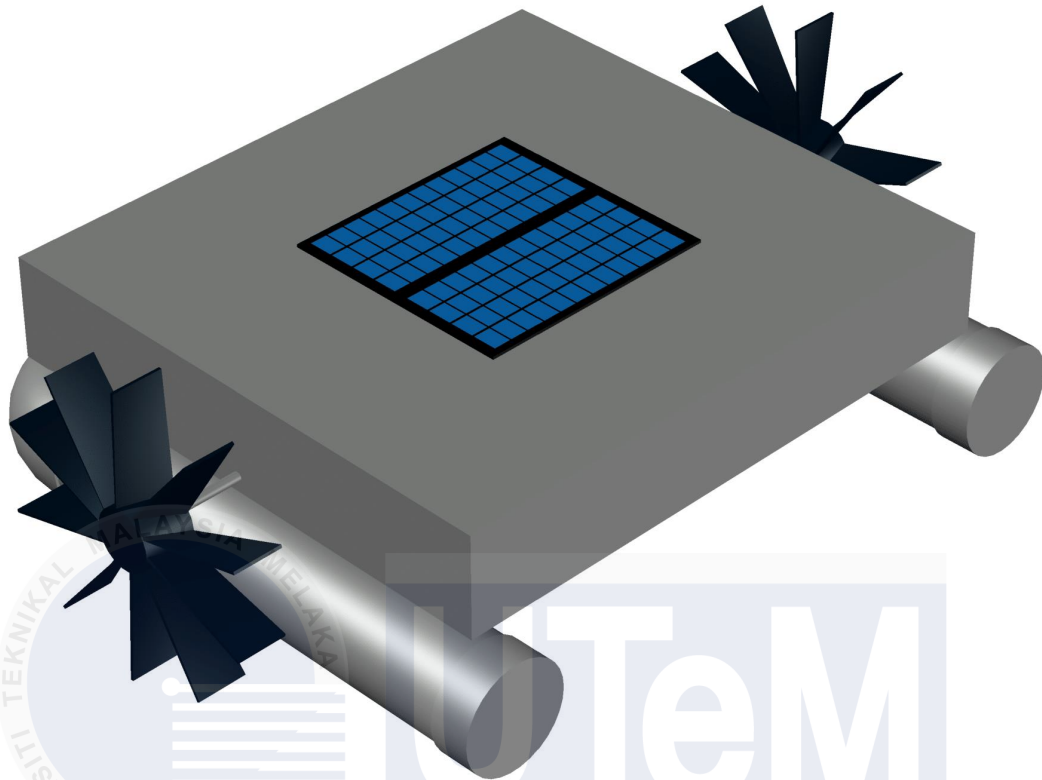


Figure 4.4 : 3D Project Design

4.3 Simulation Result

The simulation phase yielded excellent results, showcasing the project's meticulous planning and execution. To facilitate simulations, essential libraries were integrated into Proteus, a critical step in accurately emulating the system's behaviour. For instance, Arduino libraries were incorporated to simulate the robot's control mechanisms, while libraries like HC-05 were integrated to simulate Bluetooth communication. These libraries played a pivotal role in ensuring the accuracy and reliability of the simulations, providing a robust foundation for refining and optimizing the water cleaning robot's design and functionality.

4.3.1 Hc-05 Bluetooth Module

For the HC-05 Bluetooth module to establish a connection with a smartphone, it's crucial to align the port settings in the simulation with those set in the laptop's Bluetooth settings. This synchronization ensures seamless communication between the robot and the external device. Additionally, the mobile app developed using MIT App Inventor serves as an intuitive interface, enabling users to control and monitor the robot effortlessly. Figure 4.5 shown module connection in simulation.

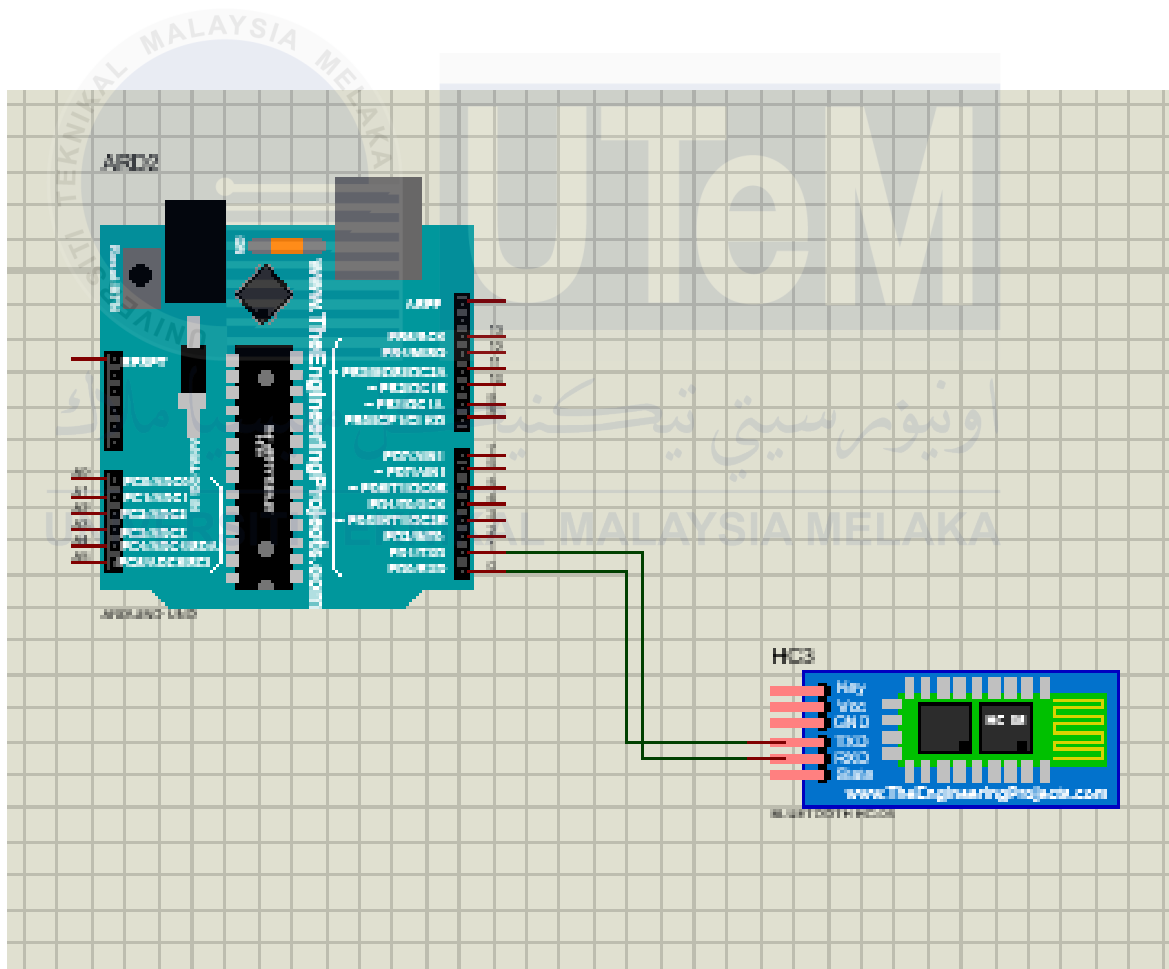


Figure 4.5 : Hc-05 in Simulation Proteus

4.3.2 Develop App Controller

By using MIT App Inventor, an app was created to control the water cleaning robot, enhancing its usability and functionality. To facilitate Bluetooth connectivity, as shown in

Figure 4.6, button was incorporated that, when pressed, lists all available devices that can connect to the robot. This feature allows users to easily select and establish a connection with the robot. Additionally, a disconnect button was added to sever the Bluetooth connection when necessary, providing a straightforward way to manage connectivity and ensuring smooth operation during different stages of use.

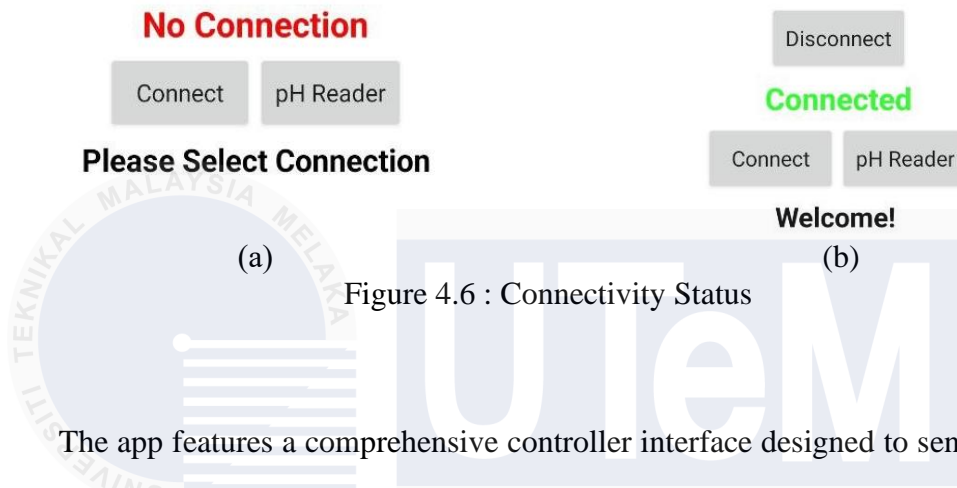


Figure 4.6 : Connectivity Status

The app features a comprehensive controller interface designed to send instructions directly to the Arduino. This interface includes buttons for various directional commands, as shown in Figure 4.7, left, right, forward, reverse, and stop. These buttons enable precise control over the robot's movements, allowing it to navigate effectively in its aquatic

environment. By providing a simple and intuitive way to manage the robot's navigation, the app enhances the overall user experience and operational efficiency.



4.3.3 Motor

The water cleaning robot employs a robust 12V DC motor, seamlessly regulated by the L298N motor driver, to facilitate precise and controlled movement. With a motor allocated to each side, the robot manoeuvres through water bodies with remarkable fluidity, effortlessly accessing confined areas and crevices for comprehensive cleaning. This versatile setup guarantees thorough sanitation across a spectrum of surfaces, reinforcing its resilience to withstand the challenges posed by demanding aquatic environments. The integration of the L298N motor driver not only ensures optimal power distribution but also enhances

operational efficiency, thereby elevating the robot's effectiveness in upholding water cleanliness standards. Figure 4.8 displays the connection dc motor in simulation.

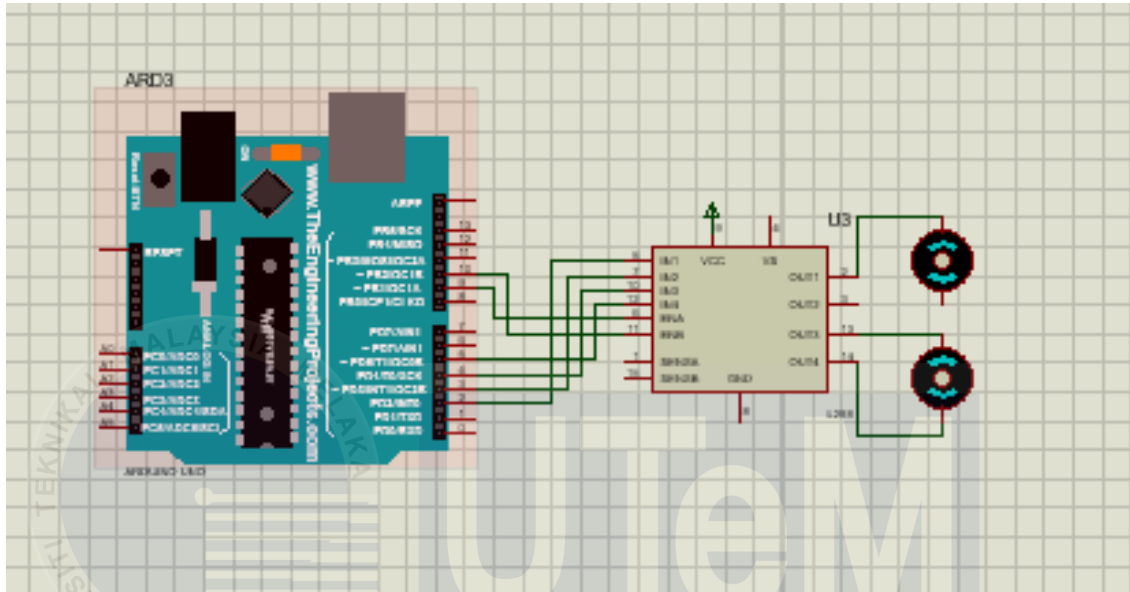


Figure 4.8 : Motor Simulation in Proteus

After conducting the simulation, the motor's operation can be observed in response to commands sent by the app. The Table 4.1 below demonstrates the results based on the specific commands transmitted. For instance, pressing the forward button within the app sends the instruction "F" to the Arduino, which then activates the motor for forward movement. Similarly, commands for left, right, and reverse movements are encoded and transmitted, resulting in the corresponding motor actions. This seamless interaction between

the app and the Arduino enables real-time control of the robot's navigation. Figure 4.9 illustrates the simulated connections used to monitor motor rotation.

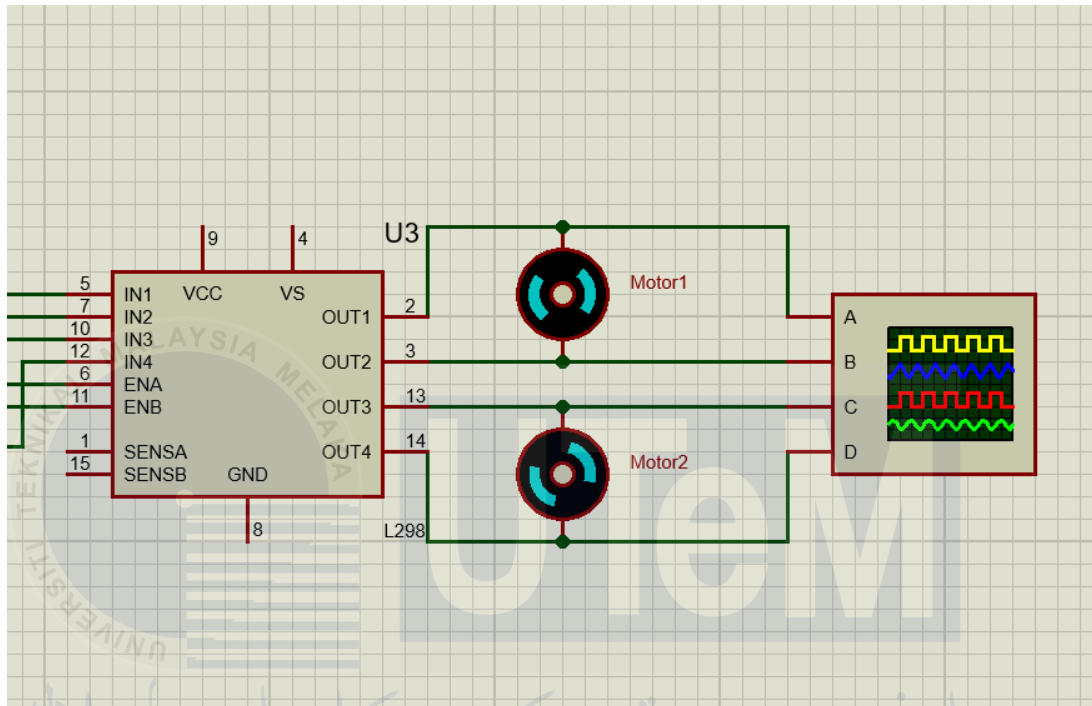
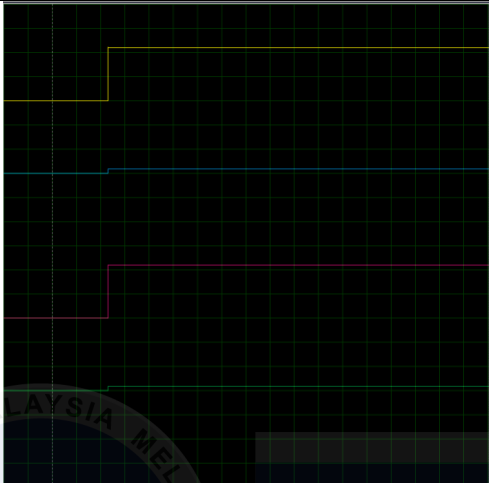
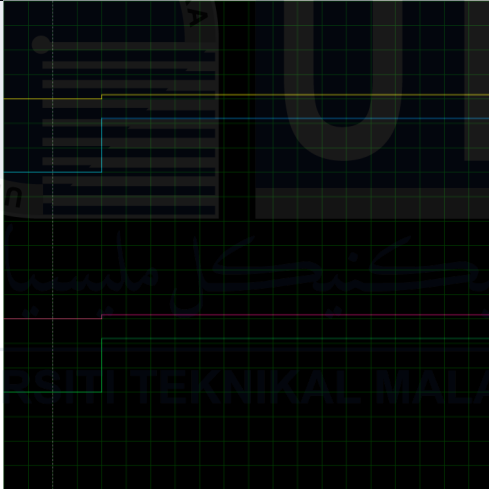
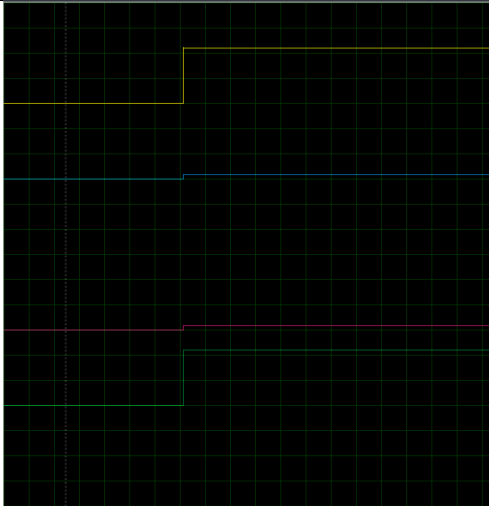
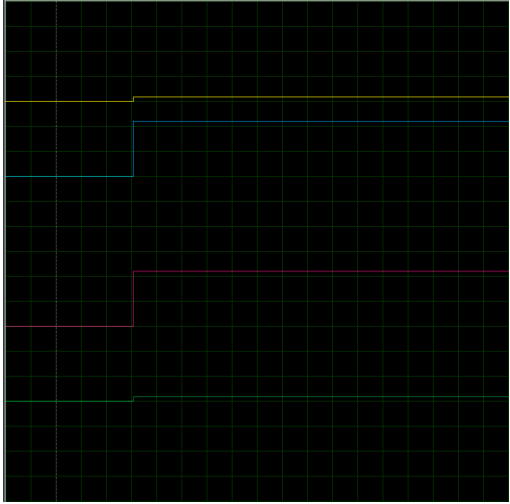


Figure 4.9 : Oscilloscope Connection

Graph lines further illustrate the motor control mechanism: yellow and blue lines represent OUT1 and OUT2 on the L298N motor driver, connected to motor1, while purple and green lines denote OUT3 and OUT4, connected to motor2.

Table 4.1 : Result for Motor Simulation

Command	Graph	Vp (V)	Motor Rotation
Forward		Out1 – 11.0 Out2 – 0.83 Out3 – 11.0 Out4 – 0.83	Motor1 – Anticlockwise Motor2 – Anticlockwise
Reverse		Out1 – 0.83 Out2 – 11.0 Out3 – 0.83 Out4 – 11.0	Motor1 – Clockwise Motor2 – Clockwise
Rigth		Out1 – 11.0 Out2 – 0.83 Out3 – 0.83 Out4 – 11.0	Motor1 – Anticlockwise Motor2 – Clockwise

Left		Out1 – 0.83 Out2 – 11.0 Out3 – 11.0 Out4 – 0.83	Motor1 – Clockwise Motor2 – Anticlockwise
------	---	--	--

Creating the app using MIT App Inventor streamlines the development process, providing a user-friendly platform for designing and implementing mobile applications. MIT App Inventor allows for intuitive drag-and-drop programming, as shown in Figure 4.10, enabling the creation of an interface that sends commands to the Arduino microcontroller. This platform facilitates the seamless integration of various functionalities, such as buttons for directional control and data displays for real-time feedback. By utilizing MIT App Inventor, the app development becomes accessible, even for those with minimal coding

experience, ultimately enhancing the overall control and interaction with the water cleaning robot.

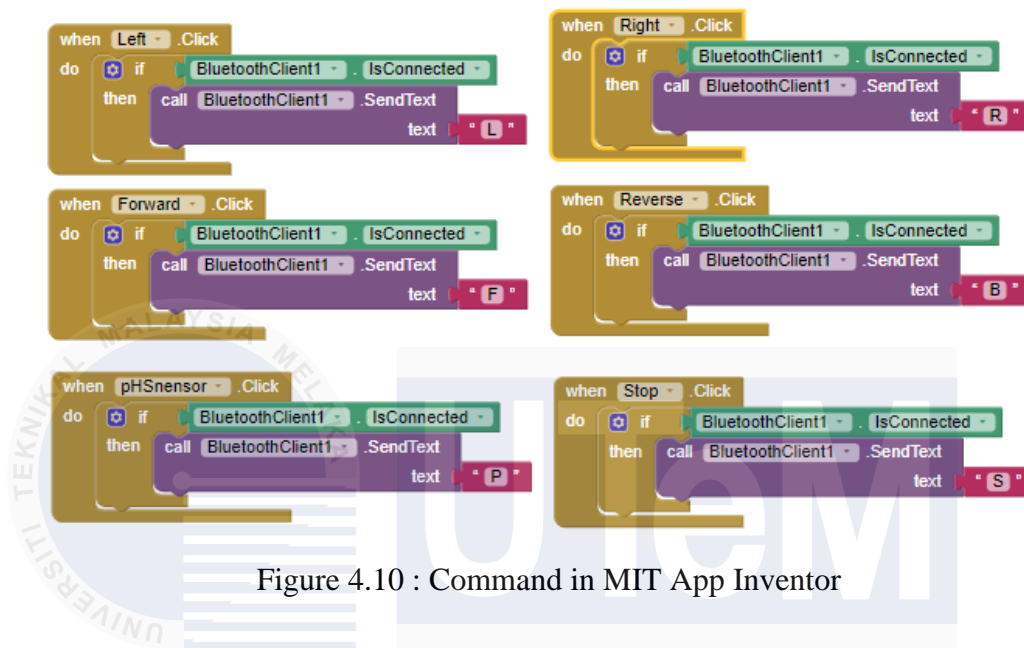


Figure 4.10 : Command in MIT App Inventor

4.3.4 Solar and Storage System

In harnessing renewable energy for power, the system incorporates an 18W solar monocrystalline panel alongside a 12V lithium-polymer (LiPo) battery. A pivotal component of this setup is the charge controller, tasked with regulating the flow of solar energy to effectively charge the battery. By interfacing between the solar panel and the battery, the charge controller ensures optimal charging efficiency while safeguarding against overcharging or undercharging, thus prolonging the battery's lifespan. This integration of solar panel, battery, and charge controller forms a sustainable energy solution, enabling reliable power generation and storage for a myriad of applications, ranging from off-grid installations to portable electronics in remote locations. Through this innovative

combination, the system harnesses clean energy, minimizing environmental impact while maximizing energy autonomy. Figure 4.11 shown the connection in simulation.

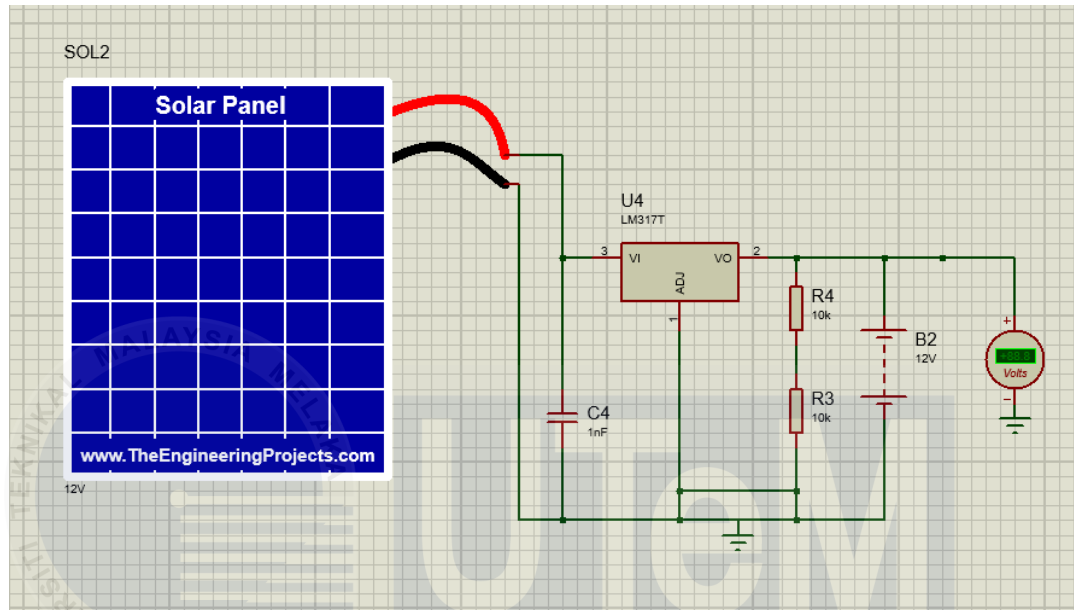


Figure 4.11 : Solar And Charge Controller Simulation in Proteus

4.4 Coding for Robot

The programming for the river water surface cleaning robot was developed using the Arduino Integrated Development Environment (IDE), a user-friendly platform widely used for microcontroller projects. The Arduino Uno, serving as the robot's microcontroller, was programmed to control key functions such as motor movements, sensor integration, and Bluetooth communication. This setup allowed the robot to effectively respond to environmental conditions and user commands sent via a mobile application. The code structure is modular and adaptable, enabling future scalability or enhancements.

For a detailed understanding of the code implementation, the complete Arduino code is included in **Appendix A**. The code is well-documented with comments explaining the functionality of each section, ensuring clarity for readers and future developers. This

comprehensive documentation facilitates easy reference and potential modifications to optimize the robot's performance.

4.4.1 Motor Command Control

In this project, the motors are controlled by an Arduino based on commands received from a Bluetooth module (HC-05). The HC-05 module receives input from a paired device, such as a smartphone, and transmits commands via serial communication to the Arduino. The Arduino processes these commands to control the motors' direction and speed using digital and PWM pins.

As shown in Figure 4.12 (a), when the letter 'F' is received, the motors rotate forward by setting the appropriate motor control pins (IN1, IN2, IN3, IN4) to make both motors spin forward. Similarly, in Figure 4.12(b) the letter 'B' reverses the motor directions to move the vehicle backward. For turning left, the 'L' command is used, which makes one motor move forward and the other reverse, while the 'R' command does the opposite to turn right as shown in Figure 4.12(c) and Figure 4.12(d).

The 'S' command stops the motors by setting all motor control pins to LOW, effectively halting the vehicle. Motor speed is controlled through PWM by setting the ENA and ENB pins with values ranging from 0 (stop) to 255 (full speed). This setup allows for

basic movement control, including forward, reverse, left, right, and stop, based on simple Bluetooth commands from the user.



```
// Control motors based on command
if (command == 'F') { // Forward

digitalWrite(IN1, HIGH);
digitalWrite(IN2, LOW);
digitalWrite(IN3, HIGH);
digitalWrite(IN4, LOW);
analogWrite(ENA, 255);
analogWrite(ENB, 255);

}

else if (command == 'B') { // Reverse

digitalWrite(IN1, LOW);
digitalWrite(IN2, HIGH);
digitalWrite(IN3, LOW);
digitalWrite(IN4, HIGH);
analogWrite(ENA, 255);
analogWrite(ENB, 255);

}

else if (command == 'L') { // Left

digitalWrite(IN1, LOW);
digitalWrite(IN2, HIGH);
digitalWrite(IN3, HIGH);
digitalWrite(IN4, LOW);
analogWrite(ENA, 255);
analogWrite(ENB, 255);

}

else if (command == 'R') { // Right

digitalWrite(IN1, HIGH);
digitalWrite(IN2, LOW);
digitalWrite(IN3, LOW);
digitalWrite(IN4, HIGH);
analogWrite(ENA, 255);
analogWrite(ENB, 255);

}

else if (command == 'S') { // Stop

digitalWrite(IN1, LOW);
digitalWrite(IN2, LOW);
digitalWrite(IN3, LOW);
digitalWrite(IN4, LOW);
analogWrite(ENA, 255);
analogWrite(ENB, 255);

}
```

(a) (b) (c) (d) (e)

Figure 4.12 : Motor Command Code

4.4.2 Command Code for LDR Sensor

The LDR (Light Dependent Resistor) sensor is used in this project to measure the ambient light intensity. The sensor is connected to the Arduino's analog pin (A0), where the Arduino continuously reads its value using `analogRead()`. When the letter 'P' is received via

the Bluetooth module, the Arduino collects multiple sensor readings to improve accuracy and reduce noise. It takes 10 samples, stores them in an array (buf[]), and then sorts the array to eliminate extreme values, keeping only the middle 6 values for averaging. Coding for LDR command as shown in Figure 4.13.

```
// Sorting the values to remove noise
for (int i = 0; i < 9; i++) {
  for (int j = i + 1; j < 10; j++) {
    if (buf[i] > buf[j]) {
      temp = buf[i];
      buf[i] = buf[j];
      buf[j] = temp;
    }
  }
}

// Average the middle 6 values for a more stable reading
avgValue = 0;
for (int i = 2; i < 8; i++) {
  avgValue += buf[i];
}
ldrValue = avgValue / 6;

// Convert LDR value to lux (you may need to adjust the calibration factor)
float lux = (ldrValue / 1023.0) * 1000.0; // This is a rough approximation.

// Output to Serial Monitor
Serial.print("Brightness: ");
Serial.print(lux, 2); // Show lux value with two decimal places
Serial.println(" lux");
```

Figure 4.13 : LDR Command Code

The average of these values is calculated to obtain a more stable reading of the LDR value. This processed value is then used to estimate the light intensity in the environment, which is displayed as the brightness in lux. The resulting lux value is printed to the serial monitor for real-time monitoring of the ambient light levels.

4.5 Physical Experiment Result

The final prototype of the solar-powered river water surface cleaning robot, as shown in Figure 4.14, has been successfully developed and tested, demonstrating its functionality

and alignment with the project objectives. The prototype features a robust design that integrates a solar panel for renewable energy harvesting, an Arduino microcontroller for precise control, and a Bluetooth module for wireless communication. The robot is equipped with a debris collection mechanism capable of efficiently gathering floating waste from water surfaces.



Figure 4.14 : Prototype Water Surface Cleaning Robot

The prototype's structure is lightweight yet durable, utilizing PVC pipes for buoyancy and a compact layout to ensure stability in aquatic environments. The solar panel is securely mounted on the top surface to optimize sunlight exposure, while a central compartment protects the electronic components from water damage. The robot's mobility is powered by dual DC motors controlled via a custom-designed mobile application, enabling seamless navigation and operation.

Extensive testing has validated the prototype's performance, confirming its ability to clean water surfaces effectively while maintaining stability and energy efficiency. This final prototype represents a significant milestone in the project, embodying a functional and

sustainable solution to water pollution. It is ready for deployment in controlled environments, with the potential for further refinement and scalability for broader applications.

4.5.1 PVC Pipe Sizing : Buoyancy Test Result

The experiment measured the submersion depth of a 2.5-inch PVC pipe under varying weight conditions. The data collected during the trials is summarized in the Table 4.2 below:

Table 4.2 : Pipe Submerged Result

Load (Kg)	Trial 1 Depth (cm)	Trial 2 Depth (cm)	Average Depth (cm)
0	2.5	2.3	2.4
1.5	4.3	4.3	4.3
3.0	6.2	6.1	6.15

The average submersion depths under each weight condition were calculated as 2.4 cm for 0 kg, 4.3 cm for 1.5 kg, and 6.15 cm for 3.0 kg to ensure consistent data

representation. In Figure 4.15, a graph to visualize the relationship between weight and submersion depth.

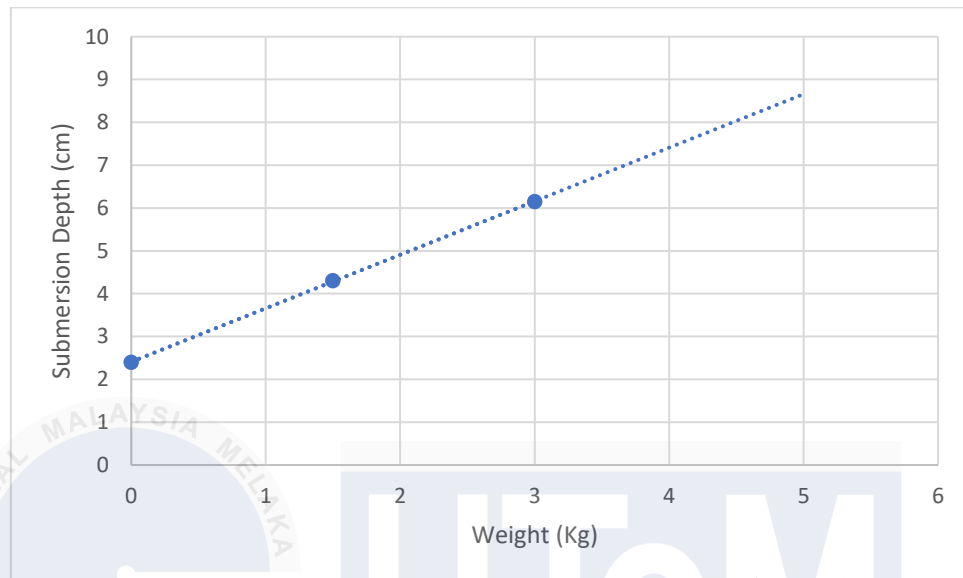


Figure 4.15 : Load Weight vs Submersion Depth

The results indicate a linear increase in submersion depth as weight increases, which is consistent with Archimedes' principle. At 0 kg, the pipe floated with a minimal submersion depth of 2.4 cm, demonstrating its inherent buoyancy. Under a load of 1.5 kg, the submersion depth increased to 4.3 cm, showing the pipe's capacity to support moderate weights. At 3.0 kg, the submersion depth reached 6.15 cm, approaching the full diameter of the pipe, indicating that it was nearing its buoyancy limit.

From these results, the 2.5-inch PVC pipe is capable of supporting up to 3 kg of weight while remaining afloat. However, for practical applications in a floating robot, it is recommended to limit the load to 2.5 kg or less to maintain stability and prevent the risk of submersion due to additional forces or uneven weight distribution.

4.5.2 Robot Cleaning Movement and Speed Result

The experiment measured the time taken by the robot to travel a distance of 3 meters under three different load conditions. The data collected during the trials is summarized in the Table 4.3 below.

Table 4.3: Robot Travel Time Results

Load (Kg)	Trial 1 Time (s)	Trail 2 Time (s)	Average Time (s)	Average Speed (m/s)
0	56	50	53.0	0.057
1.5	78	82	80.0	0.038
3.0	90	93	91.5	0.033

The average travel times for each load condition were calculated as 53.0 seconds for 0 kg, 80.0 seconds for 1.5 kg, and 91.5 seconds for 3.0 kg to ensure consistent data representation. The corresponding average speeds were determined as 0.057 m/s for 0 kg,

0.038 m/s for 1.5 kg, and 0.033 m/s for 3.0 kg. In Figure 4.16 show graph load weight versus speed.

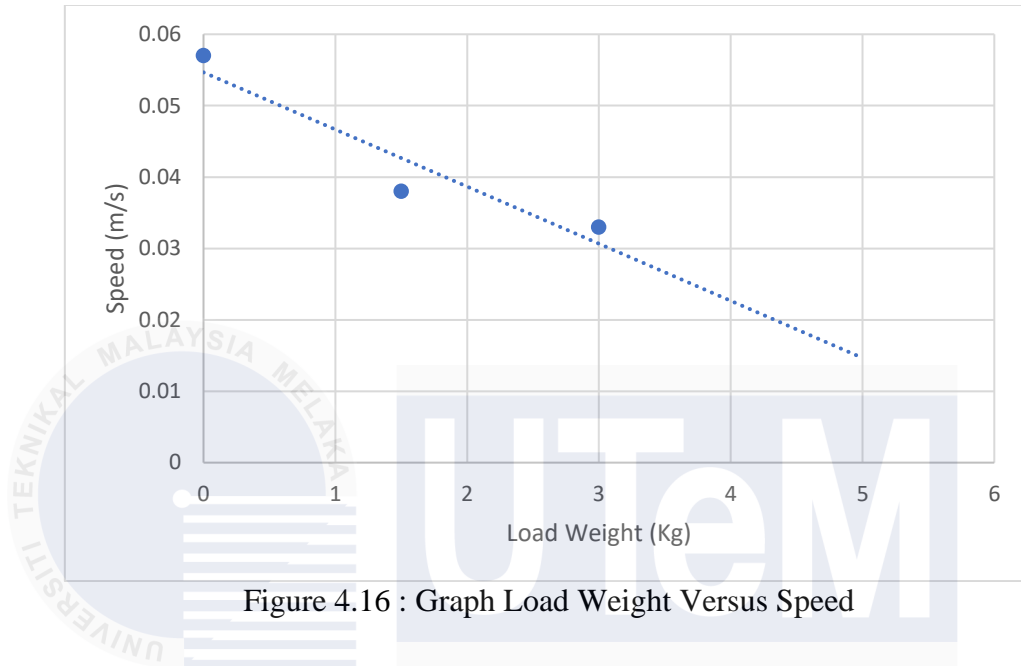


Figure 4.16 : Graph Load Weight Versus Speed

The results indicate that the robot's travel time increased as the load increased, corresponding to a reduction in speed. With no load (0 kg), the robot completed the 3-meter distance in 53.0 seconds, achieving an average speed of 0.057 m/s, which represents its maximum speed under ideal conditions. Under a 1.5 kg load, the travel time increased to 80.0 seconds, with the speed decreasing to 0.038 m/s, suggesting moderate weight handling with minimal performance impact. At a 3.0 kg load, the travel time reached 91.5 seconds, and the speed dropped further to 0.033 m/s, indicating a significant reduction in speed due to the additional weight.

From these results, it can be concluded that the robot performs efficiently with a load of up to 3.0 kg, maintaining acceptable speeds. However, for practical applications, it is recommended to limit the load to 2.5 kg or less to ensure optimal performance. This

precaution minimizes strain on the robot's motor and components, avoiding reduced efficiency or potential mechanical failure over time.

4.5.3 HC05 Bluetooth Signal Limit Distance Result

The experiment measured the effective communication range of the DHT11 sensor when paired with a receiver. The data collected during the trials is summarized in the Table 4.4 below.

Table 4.4 : DHT11 Communication Distance Results

Distance (m)	Buzzer Status
5	ON
10	ON
15	ON
17	Start Lost Signal
20	OFF

Reliable communication was determined as the furthest distance at which the HC-05 Bluetooth module consistently activated the buzzer in all three trials. This value was compared across all tested distances to identify the module's effective range.

The results indicate that the HC-05 Bluetooth module maintained reliable communication up to 15 meters, with the buzzer consistently turning on at this distance. Beyond 15 meters, intermittent signal loss began at 17 meters, and the module failed to activate the buzzer at 20 meters, indicating complete signal loss.

From these results, the maximum effective communication distance of the HC-05 Bluetooth module was identified as 15 meters. This provides valuable insights into the module's operational limitations for wireless communication applications. For practical use, it is recommended to deploy the module within a distance slightly shorter than 15 meters to ensure reliable signal transmission, accounting for potential environmental interferences or signal degradation over time.

4.5.4 Effect of Sun brightness, temperature and Humidity toward solar efficiency

Result

The results of the experiment were analysed to determine the impact of sun brightness, temperature, and humidity on the solar panel's efficiency. The data collected during the trials is summarized in the Table 4.5 below.

Table 4.5 : Solar Panel Efficiency Under Different Environmental Conditions

Time of Day	Sun Brightness (Lux)	Temperature (°C)	Humidity (%)	Output Voltage (V)
8:00 AM	9032	26	80	9.4
9:00 AM	12341	27.5	78	10.0
10:00 AM	18124	29	76	10.8
11:00 AM	25432	31	74	11.5
12:00 PM	31095	33	73	12.5
1:00 PM	35217	35	72	13.2
2:00 PM	34574	34.5	72.5	13.2
3:00 PM	30665	33	73	12.5
4:00 PM	25433	31	74	11.8
5:00 PM	12743	30	75	11.2
6:00 PM	12634	30	75	11.0

The output voltage of the solar panel varies throughout the day, following a distinct daily pattern. In the morning at 8:00 AM, the output voltage starts at 9.4 V and increases steadily as the day progresses, reaching its peak of 13.2 V at 1:00 PM. Afterward, the voltage begins to decrease, ending at 11.0 V by 6:00 PM. This trend correlates with the availability of sunlight throughout the day, as the intensity of sunlight generally increases in the morning, peaks in the afternoon, and diminishes in the evening. In Figure 4.17, a graph plotting time on the x-axis and output voltage on the y-axis would illustrate this trend, showing a bell-

shaped curve with the peak in the early afternoon. This relationship emphasizes how solar panel performance is directly tied to the daily solar cycle.

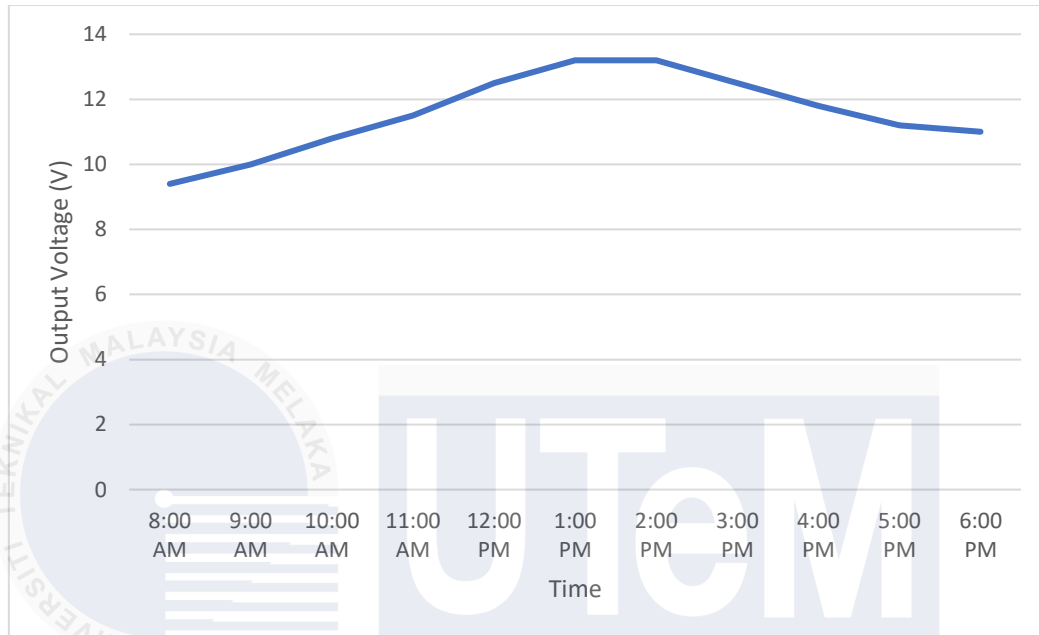


Figure 4.17 : Time vs. Output Voltage

The relationship between sun brightness and output voltage is strongly positive. As sun brightness increases, the output voltage also rises, reaching its maximum at the highest brightness of 35,217 Lux at 1:00 PM. A minor deviation occurs at 2:00 PM, where the brightness slightly decreases to 34,574 Lux, but the output remains at 13.2 V. This suggests that the solar panel's output voltage is highly dependent on sunlight intensity, as brighter conditions provide more energy for the photovoltaic cells to convert. A graph plotting sun brightness on the x-axis and output voltage on the y-axis would show a steep increase up to the peak, followed by a gradual decline. This strong

correlation highlights the importance of optimal sunlight exposure for maximizing solar panel efficiency.

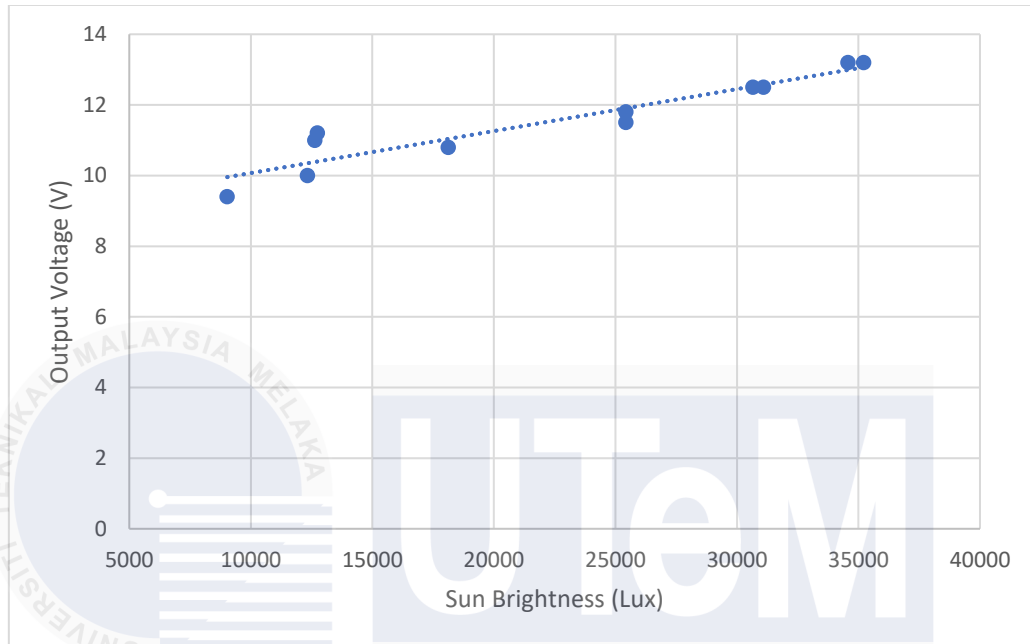


Figure 4.18 : Sun Brightness vs. Output Voltage

Temperature also shows a positive correlation with output voltage. The voltage rises as the temperature increases, peaking at 35°C, corresponding to the highest output voltage of 13.2 V. Beyond this point, even when the temperature remains high at 34.5°C, the output voltage stabilizes rather than increases further. This indicates that while temperature contributes to improving solar efficiency, it may have diminishing returns or even adverse effects at higher levels. A graph plotting temperature on the x-axis and output voltage on the y-axis in Figure 4.17. This relationship suggests that maintaining an optimal temperature range is important for sustaining peak performance.

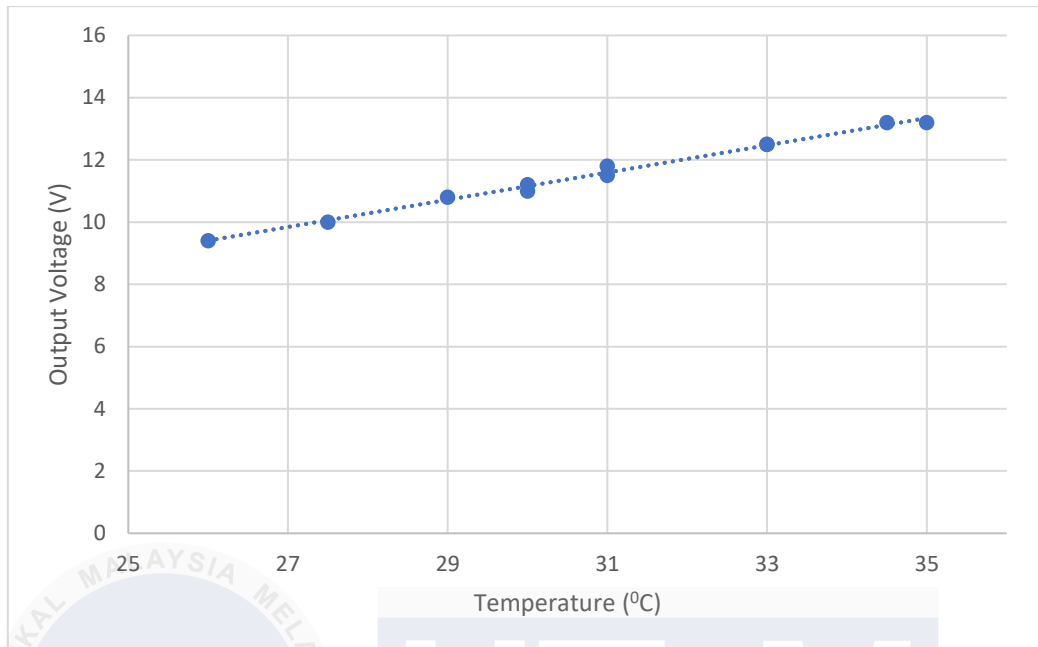


Figure 4.19 : Temperature vs. Output Voltage

Humidity exhibits an inverse relationship with output voltage, albeit less pronounced than the effects of sunlight and temperature. At higher humidity levels, such as 80% in the morning at 8:00 AM, the output voltage is lower (9.4 V). Conversely, when humidity drops to its lowest level of 72% at 1:00 PM, the output voltage reaches its peak of 13.2 V. This trend suggests that higher humidity may reduce solar panel efficiency, possibly due to light scattering or condensation reducing sunlight absorption. A graph plotting humidity on the x-

axis and output voltage on the y-axis in Figure 4.18, reinforcing the idea that lower humidity supports better performance.

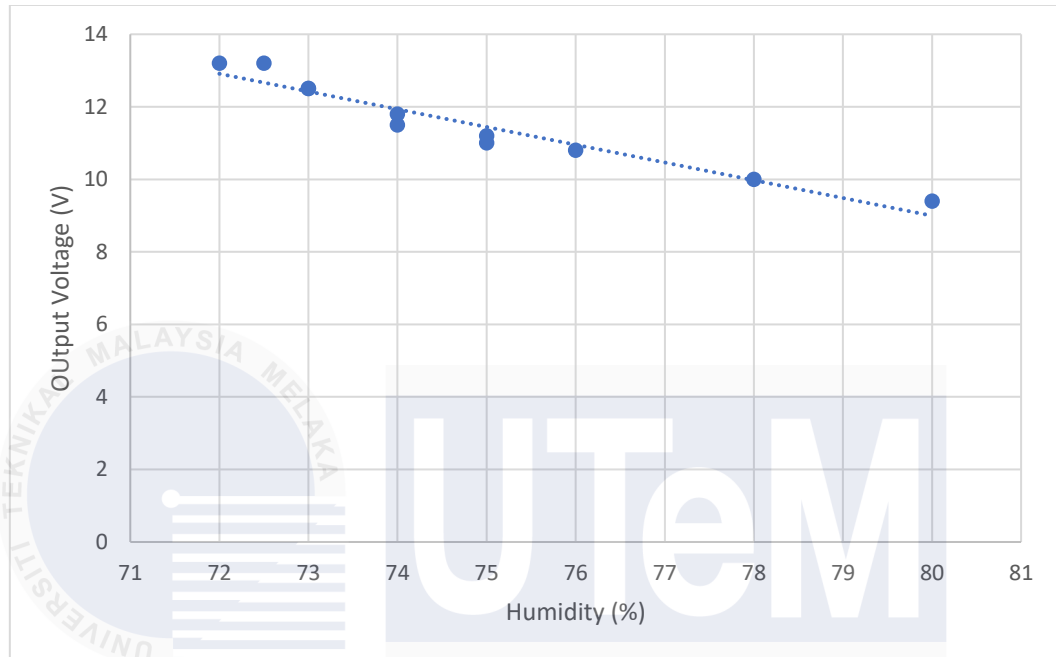


Figure 4.20 : Humidity vs. Output Voltage

The data demonstrate that the solar panel's performance, indicated by its output voltage, is significantly influenced by environmental factors. Sunlight intensity is the primary driver of efficiency, with the highest brightness resulting in the maximum voltage. Temperature also positively impacts output voltage, but with diminishing returns at higher levels. Humidity plays a minor role, with lower humidity levels slightly enhancing efficiency. Overall, the solar panel performs best under conditions of high sunlight intensity, moderate to high temperatures, and low humidity. This analysis underscores the importance of environmental factors in determining the real-world efficiency of solar panels.

4.5.5 Motor rotation speed Result

The experiment measured the number of rotations completed by the motor in one minute at a fixed input voltage of 12V. The data collected during the trials is summarized in the Table 4.6 below:

Table 4.6 : Motor Rotational Speed Results

Trial	Total Rotation
1	5
2	6
3	6
Average	5.67

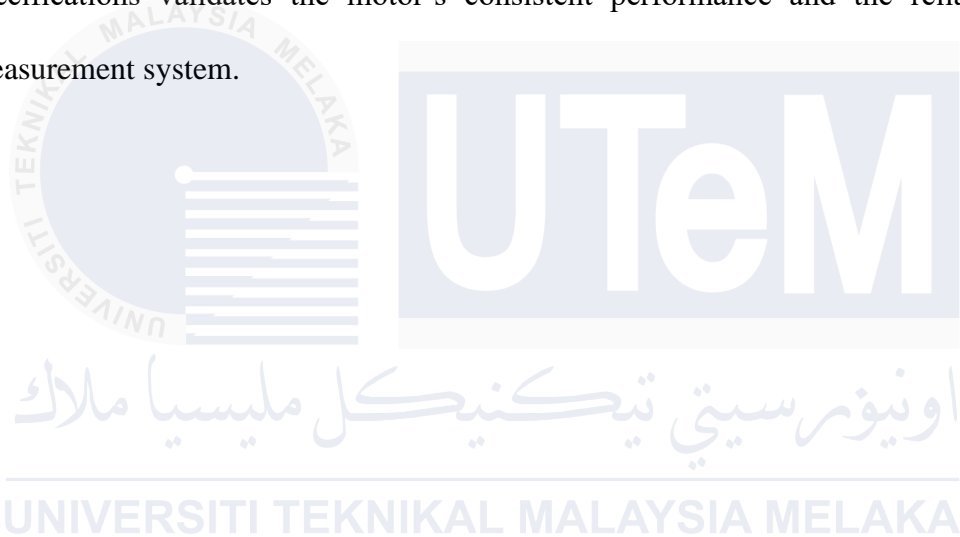
The average rotational speed (RPM) was calculated by taking the mean of the total rotations recorded across the three trials. The calculated average RPM is 5.67 rotations per minute.

The results show that the motor maintained consistent performance across all three trials, with minimal variation in the number of rotations recorded. The slight variation between trials—ranging from 5 to 6 rotations—demonstrates the stability of the motor at a fixed voltage of 12V and confirms the reliability of the IR sensor and handmade encoder in measuring rotational speed.

Minor deviations observed between trials may have been caused by factors such as slight misalignments of the encoder disk, variations in the motor's operation, or

environmental factors affecting the IR sensor's accuracy. Despite these small variations, the overall results were consistent, supporting the accuracy of the system.

The calculated average RPM provides valuable insight into the motor's performance under controlled conditions. The motor's RPM, which averaged 5.67 rotations per minute, is almost the same as the 6 RPM claimed in the motor's datasheet, confirming that the motor performs as expected. This alignment between the experimental results and the datasheet specifications validates the motor's consistent performance and the reliability of the measurement system.



CHAPTER 5

CONCLUSION AND RECOMMENDATIONS

5.1 Conclusion

In reflecting on the extensive progress attained throughout the developmental phases of the water cleaning robot, it is immensely gratifying to acknowledge the resounding success achieved in meeting all outlined objectives. From the meticulous planning stages, where each component's intricacies were meticulously mapped out, to the rigorous testing procedures undertaken to ensure optimal functionality, the unwavering dedication of the team has culminated in the realization of an exceptionally functional and efficient solution. The integration of cutting-edge technologies, notably the utilization of Arduino as the motor controller for precise and responsive movement, has been pivotal in ensuring thorough cleaning across a diverse array of water surfaces. Furthermore, the strategic implementation of the HC-05 Bluetooth module and the adept crafting of a bespoke application utilizing MIT App Inventor have significantly enriched user accessibility and control, thereby amplifying the robot's efficacy in navigating real-world environments.

Moreover, the seamless execution of simulations stands as a testament to the robustness and reliability inherent within our meticulously crafted design. Through meticulous validation processes, we have fortified our confidence in the solution's capability to address pressing environmental concerns with unwavering efficacy. By harnessing renewable energy sources such as the solar monocrystalline panel and the 12V LiPo battery, we not only guarantee sustainable operation but also underscore our profound commitment to championing environmentally conscious practices. As we stand on the precipice of

transitioning from the developmental phase to the deployment stage, we are brimming with anticipation and optimism about the transformative impact our water cleaning robot will inevitably wield in tackling the paramount challenges faced by our ecosystems. This journey signifies not merely a technological milestone but a monumental stride toward fostering a cleaner, healthier, and more sustainable future for our shared planet. Environmental concerns. This journey signifies not just a technological achievement but also a step forward towards a cleaner and healthier future for our planet.

5.2 Future Works

Future work on the project can focus on advancing the robot's capabilities and expanding its applicability. Integrating autonomous navigation systems, such as GPS or machine learning algorithms, would enable self-sufficient operation and efficient obstacle avoidance. Expanding sensor integration to measure additional water quality parameters like turbidity and dissolved oxygen could provide more comprehensive monitoring.

Scaling the design for use in larger water bodies and exploring deployment opportunities with environmental agencies could amplify its impact. Investigating lightweight, durable materials could further improve buoyancy and energy efficiency, while incorporating advanced battery technologies or hybrid energy systems could extend operational hours during low sunlight. These developments would significantly enhance the

robot's performance and solidify its role as an innovative solution for sustainable water surface cleaning.

Enhance the user experience and functionality of the app interface through iterative design iterations and user feedback integration. By refining the user interface, streamlining navigation pathways, and introducing new features or functionalities, we aim to optimize user engagement, accessibility, and control. This iterative approach to app development ensures that the interface remains intuitive, user-friendly, and responsive, aligning seamlessly with the evolving needs and preferences of end-users.

Through a concerted focus on these future work areas, we are poised to elevate the water cleaning robot project to new heights of innovation, functionality, and impact. By prioritizing hardware realization, refining project weaknesses, and enhancing app interface design, we position ourselves at the forefront of environmental stewardship, driving positive change and sustainability in water sanitation efforts.

REFERENCES

- [1] “Melaka and George Town, Historic Cities of the Straits of Malacca,” *World Herit. Conv.*, [Online]. Available: <https://whc.unesco.org/en/list/1223/>
- [2] P. Kannan, “STATISTIK KEDATANGAN PELANCONG KE NEGERI MELAKA,” 2020.
- [3] “MGF24032021_HUMANINTERESTASIK_07-copy-1024x684.” Malaysia Gazette. [Online]. Available: <https://malaysiagazette.com/2021/03/24/kerja-kerja-pembersihan-di-tasik-putrajaya/>
- [4] Z. Wu, T. S. Adebayo, and A. A. Alola, “Renewable energy intensity and efficiency of fossil energy fuels in the nordics: How environmentally efficient is the energy mix?,” *J. Clean. Prod.*, vol. 438, 2024, doi: 10.1016/j.jclepro.2024.140711.
- [5] R. Sampedro, “The Sustainable Development Goals (SDG),” *Carreteras*, vol. 4, no. 232, 2021, doi: 10.4324/9780429282348-52.
- [6] D. H. Autor, “Why are there still so many jobs? the history and future of workplace automation,” in *Journal of Economic Perspectives*, 2015. doi: 10.1257/jep.29.3.3.
- [7] C. Alonso, A. Berg, S. Kothari, C. Papageorgiou, and S. Rehman, “Will the AI revolution cause a great divergence?,” *J. Monet. Econ.*, vol. 127, 2022, doi: 10.1016/j.jmoneco.2022.01.004.
- [8] S. Benbernou, “Factorization model of robotic tasks,” *Artif. Intell. Eng.*, vol. 13, no. 1, 1999, doi: 10.1016/S0954-1810(98)00001-6.
- [9] D. H. Kim, G. M. Park, Y. H. Yoo, S. J. Ryu, I. B. Jeong, and J. H. Kim, “Realization of task intelligence for service robots in an unstructured environment,” *Annual Reviews in Control*, vol. 44. 2017. doi: 10.1016/j.arcontrol.2017.09.013.
- [10] A. Vysocky and P. Novak, “HUMAN – ROBOT COLLABORATION IN

- INDUSTRY,” no. June 2016, 2017, doi: 10.17973/MMSJ.2016.
- [11] H. Bhattarai, “Renewable energy and energy storage systems,” *Energy Convers. Methods, Technol. Futur. Dir.*, pp. 269–289, 2022, doi: 10.52305/wxnj6607.
- [12] B. Raybould, W. M. Cheung, C. Connor, and R. Butcher, “An investigation into UK government policy and legislation to renewable energy and greenhouse gas reduction commitments,” *Clean Technol. Environ. Policy*, vol. 22, no. 2, 2020, doi: 10.1007/s10098-019-01786-x.
- [13] U. S. E. I. Administration, “U.S. energy production and consumption in 2023 - Renewable Energy,” *Adm. U.S. Energy Inf.*, 2024, [Online]. Available: <https://www.eia.gov/tools/faqs/faq.php?id=92&t=4>
- [14] S. Glomsrød, T. Wei, and K. H. Alfsen, “Pledges for climate mitigation: The effects of the Copenhagen accord on CO₂ emissions and mitigation costs,” *Mitig. Adapt. Strateg. Glob. Chang.*, vol. 18, no. 5, 2013, doi: 10.1007/s11027-012-9378-2.
- [15] Q. M. Tran, “Projection of fossil fuel demands in Vietnam to 2050 and climate change implications,” *Asia Pacific Policy Stud.*, vol. 6, no. 2, 2019, doi: 10.1002/app5.274.
- [16] U. S. E. I. Administration, “Renewable Energy Consumption and Electricity Preliminary Statistics 2010,” *Renew. Energy*, no. June 2011, p. 13, 2011, [Online]. Available: <http://www.eia.gov/renewable/annual/preliminary/pdf/preliminary.pdf>
- [17] S. Shafiee and E. Topal, “A long-term view of worldwide fossil fuel prices,” *Appl. Energy*, vol. 87, no. 3, 2010, doi: 10.1016/j.apenergy.2009.09.012.
- [18] L. Shaw, J. Pratt, L. Klebanoff, T. Johnson, M. Arienti, and M. Moreno, “Analysis of H₂ storage needs for early market ‘man-portable’ fuel cell applications,” *Int. J. Hydrogen Energy*, vol. 38, no. 6, 2013, doi: 10.1016/j.ijhydene.2012.12.066.

- [19] M. Perez and R. Perez, "Update 2022 – A fundamental look at supply side energy reserves for the planet," *Sol. Energy Adv.*, vol. 2, 2022, doi: 10.1016/j.seja.2022.100014.
- [20] B. Parida, S. Iniyar, and R. Goic, "A review of solar photovoltaic technologies," *Renewable and Sustainable Energy Reviews*, vol. 15, no. 3, 2011. doi: 10.1016/j.rser.2010.11.032.
- [21] L. A. Dobrzański, A. Drygała, M. Giedroć, and M. Macek, "Monocrystalline silicon solar cells applied in photovoltaic system," *Monocrystalline silicon Sol. cells Appl. Photovolt. Syst.*, vol. 53, no. 1, pp. 7–13, 2012.
- [22] M. A. Bashir, H. M. Ali, S. Khalil, M. Ali, and A. M. Siddiqui, "Comparison of performance measurements of photovoltaic modules during winter months in Taxila, Pakistan," *Int. J. Photoenergy*, vol. 2014, 2014, doi: 10.1155/2014/898414.
- [23] "Types of Solar Panels," GreenMatch. [Online]. Available: <https://www.greenmatch.co.uk/blog/2015/09/types-of-solar-panels>
- [24] Catherine Lane, "Types of solar panels: which one is the best choice?," SolarReviews. [Online]. Available: <https://www.solarreviews.com/blog/pros-and-cons-of-monocrystalline-vs-polycrystalline-solar-panels>
- [25] T. Niewelt *et al.*, "Taking monocrystalline silicon to the ultimate lifetime limit," *Sol. Energy Mater. Sol. Cells*, vol. 185, 2018, doi: 10.1016/j.solmat.2018.05.040.
- [26] T. Kato, J. L. Wu, Y. Hirai, H. Sugimoto, and V. Bermudez, "Record Efficiency for Thin-Film Polycrystalline Solar Cells Up to 22.9% Achieved by Cs-Treated Cu(In,Ga)(Se,S)₂," *IEEE J. Photovoltaics*, vol. 9, no. 1, 2019, doi: 10.1109/JPHOTOV.2018.2882206.
- [27] I. Hajdukovic, "The impact of international trade on the price of solar photovoltaic modules: empirical evidence," *Economia*, vol. 23, no. 1, 2022, doi: 10.1108/ECON-

05-2022-0007.

- [28] Solar Magazine, "Monocrystalline vs Polycrystalline Solar Panels," *Sol. Mag.*, pp. 1–16, 2020.
- [29] M. V. Dambhare, B. Butey, and S. V. Moharil, "Solar photovoltaic technology: A review of different types of solar cells and its future trends," *J. Phys. Conf. Ser.*, vol. 1913, no. 1, pp. 0–16, 2021, doi: 10.1088/1742-6596/1913/1/012053.
- [30] B. Lutkevich, "What is a Microcontroller and How Does it Work?," *IoT Agenda*, no. 1c, 2019.
- [31] N. Wang, "Basic Microcontroller Use for Measurement and Control," *Basic Microcontroller Use Meas. Control*, 2020, doi: 10.21061/introbiosystemsengineering/microcontroller.
- [32] Arduino.cc, "Arduino Uno Rev3," *Arduino.Cc*, 2020.
- [33] R. Mischianti, "Arduino UNO Rev 3: high-resolution pinout, datasheet, and specs," 2023, [Online]. Available: <https://mischianti.org/arduino-uno-rev-3-high-resolution-pinout-datasheet-and-specs/>
- [34] K. H. Chao and B. Z. Huang, "Quantitative Design for the Battery Equalizing Charge/Discharge Controller of the Photovoltaic Energy Storage System," *Batteries*, vol. 8, no. 12, 2022, doi: 10.3390/batteries8120278.
- [35] M. Oswal, J. Paul, and R. Zhao, "A Comparative Study of Lithium-Ion Batteries.," *Univ. South. Calif.*, p. 31, 2010, [Online]. Available: http://www-scf.usc.edu/~rzhao/LFP_study.pdf
- [36] A. Gibbs, "The Gibbs Guide to Lithium Polymer Batteries By," pp. 1–67, 2013.
- [37] G. Albright, J. Edie, and S. Al-Hallaj, "A Comparison of Lead Acid to Lithium-ion in Stationary Storage Applications," *AllCell Technol. LLC*, no. March, p. 14, 2012.

- [38] A. K. Shukla, S. Venugopalan, and B. Hariprakash, "Nickel-based rechargeable batteries," *J. Power Sources*, vol. 100, no. 1–2, 2001, doi: 10.1016/S0378-7753(01)00890-4.
- [39] K. Rose, D. Kelly, C. Kemker, K. Fitch, and A. Car, "pH of Water Fundamentals of Environmental Measures," Fondriest Environmental Inc.
- [40] V. K. Manam and S. Nanoparticles, "TRENDS IN Weser Books," no. September, 2022.
- [41] J. Herrmann, E. Degerman, A. Gerhardt, C. Johansson, P. E. Lingdell, and I. P. Muniz, "Acid-stress effects on stream biology," *Ambio*, vol. 22, no. 5, pp. 298–307, 1993.
- [42] S. Vajpayee, B. Kumar, R. Thakur, and M. Kumar, "Design and Development of Nano pH Sensor and Interfacing with Arduino," *Des. Dev. Nano pH Sens. Interfacing with Arduino Des. Dev. Nano pH Sens. Interfacing with Arduino*, vol. 6, no. 4, pp. 66–75, 2017.
- [43] e-Gizmo Mechatronix Central, "PH Sensor E-201-C." pp. 1–8, 2017.
- [44] Siddhanna Janai, "Swachh Hasth-A Water Cleaning Robot," *Int. J. Eng. Res.*, vol. V9, no. 07, pp. 839–842, 2020, doi: 10.17577/ijertv9is070377.
- [45] N. A. S. Kamarudin, I. N. A. M. Nordin, D. Misman, N. Khamis, M. R. M. Razif, and F. H. M. Noh, "Development of Water Surface Mobile Garbage Collector Robot," *Alinteri J. Agric. Sci.*, vol. 36, no. 1, pp. 534–540, 2021, doi: 10.47059/alinteri/v36i1/ajas21076.
- [46] E. Rahmawati, I. Sucahyo, A. Asnawi, M. Faris, M. A. Taqwim, and D. Mahendra, "A Water Surface Cleaning Robot," *J. Phys. Conf. Ser.*, vol. 1417, no. 1, 2019, doi: 10.1088/1742-6596/1417/1/012006.

- [47] S. Farina, H. Zabidi, H. A. Kadir, and M. Danial, “Real-Time Monitoring System for an Aquatic Surface Cleaning Robot using MIT App Inventor,” *Evol. Electr. Electron. Eng.*, vol. 2, no. 2, pp. 677–685, 2021, [Online]. Available: <http://publisher.uthm.edu.my/periodicals/index.php/eeee>
- [48] M. Balu, P. Chowla, P. S. Middela, and H. Bestha, “Design and Development of a Solar-Powered Vacuum and Wet Cleaning Robot using Arduino UNO,” *Int. J. Inf. Technol. Infrastruct.*, vol. 12, no. 3, pp. 1–4, 2023, doi: 10.30534/ijiti/2023/011232023.



APPENDICES

Appendix A

Full Code For Arduino Uno

```
[1] // Variable Declarations
[2] char command;
[3] int ldrValue;
[4] int buf[10], temp;
[5] unsigned long int avgValue;
[6]
[7] // Pin Definitions
[8] #define SensorPin A0
[9] #define ENA 9
[10] #define ENB 10
[11] #define IN1 2
[12] #define IN2 3
[13] #define IN3 4
[14] #define IN4 5
[15]
[16] // Setup Function
[17] void setup() {
[18]     // Initialize serial communication
[19]     Serial.begin(9600);
[20]     Serial.println("Welcome!");
[21]
[22]     // Initialize motor control pins
[23]     pinMode(IN1, OUTPUT);
[24]     pinMode(IN2, OUTPUT);
[25]     pinMode(IN3, OUTPUT);
[26]     pinMode(IN4, OUTPUT);
[27]     pinMode(ENA, OUTPUT);
[28]     pinMode(ENB, OUTPUT);
[29]
[30]     // Initialize motors to be off
[31]     digitalWrite(IN1, LOW);
[32]     digitalWrite(IN2, LOW);
[33]     digitalWrite(IN3, LOW);
[34]     digitalWrite(IN4, LOW);
[35]     analogWrite(ENA, 0);
[36]     analogWrite(ENB, 0);
[37] }
```

```

[38]
[39] // Main Loop Function
[40] void loop() {
[41]     // Check if data is available to read
[42]     if (Serial.available() > 0) {
[43]         command = Serial.read(); // Read the incoming data
[44]
[45]         // Control motors based on command
[46]         if (command == 'F') { // Forward
[47]             digitalWrite(IN1, HIGH);
[48]             digitalWrite(IN2, LOW);
[49]             digitalWrite(IN3, HIGH);
[50]             digitalWrite(IN4, LOW);
[51]             analogWrite(ENA, 255);
[52]             analogWrite(ENB, 255);
[53]         } else if (command == 'B') { // Reverse
[54]             digitalWrite(IN1, LOW);
[55]             digitalWrite(IN2, HIGH);
[56]             digitalWrite(IN3, LOW);
[57]             digitalWrite(IN4, HIGH);
[58]             analogWrite(ENA, 255);
[59]             analogWrite(ENB, 255);
[60]         } else if (command == 'L') { // Left
[61]             digitalWrite(IN1, LOW);
[62]             digitalWrite(IN2, HIGH);
[63]             digitalWrite(IN3, HIGH);
[64]             digitalWrite(IN4, LOW);
[65]             analogWrite(ENA, 255);
[66]             analogWrite(ENB, 255);
[67]         } else if (command == 'R') { // Right
[68]             digitalWrite(IN1, HIGH);
[69]             digitalWrite(IN2, LOW);
[70]             digitalWrite(IN3, LOW);
[71]             digitalWrite(IN4, HIGH);
[72]             analogWrite(ENA, 255);
[73]             analogWrite(ENB, 255);
[74]         } else if (command == 'S') { // Stop
[75]             digitalWrite(IN1, LOW);
[76]             digitalWrite(IN2, LOW);
[77]             digitalWrite(IN3, LOW);
[78]             digitalWrite(IN4, LOW);
[79]             analogWrite(ENA, 255);
[80]             analogWrite(ENB, 255);

```

```

[81]     } else if (command == 'P') { // Light Intensity Measurement
[82]         for (int i = 0; i < 10; i++) {
[83]             buf[i] = analogRead(SensorPin);
[84]             delay(10);
[85]         }
[86]
[87]         // Sorting the values to remove noise
[88]         for (int i = 0; i < 9; i++) {
[89]             for (int j = i + 1; j < 10; j++) {
[90]                 if (buf[i] > buf[j]) {
[91]                     temp = buf[i];
[92]                     buf[i] = buf[j];
[93]                     buf[j] = temp;
[94]                 }
[95]             }
[96]         }
[97]
[98]         // Average the middle 6 values for a stable reading
[99]         avgValue = 0;
[100]        for (int i = 2; i < 8; i++) {
[101]            avgValue += buf[i];
[102]        }
[103]        ldrValue = avgValue / 6;
[104]
[105]        // Convert LDR value to lux (adjust the calibration factor as needed)
[106]        float lux = (ldrValue / 1023.0) * 1000.0;
[107]
[108]        // Output to Serial Monitor
[109]        Serial.print("Brightness: ");
[110]        Serial.print(lux, 2); // Display lux value with two decimal places
[111]        Serial.println(" lux");
[112]    }
[113] }
}

```